

ES18: Electronic Structure Workshop

-- hosted by U. Penn



*****Perspectives on the Projector Augmented Wave Method (PAW)*****

**Natalie A. W. Holzwarth, Wake Forest University,
Department of Physics, Winston-Salem, NC, USA**

Acknowledgements:

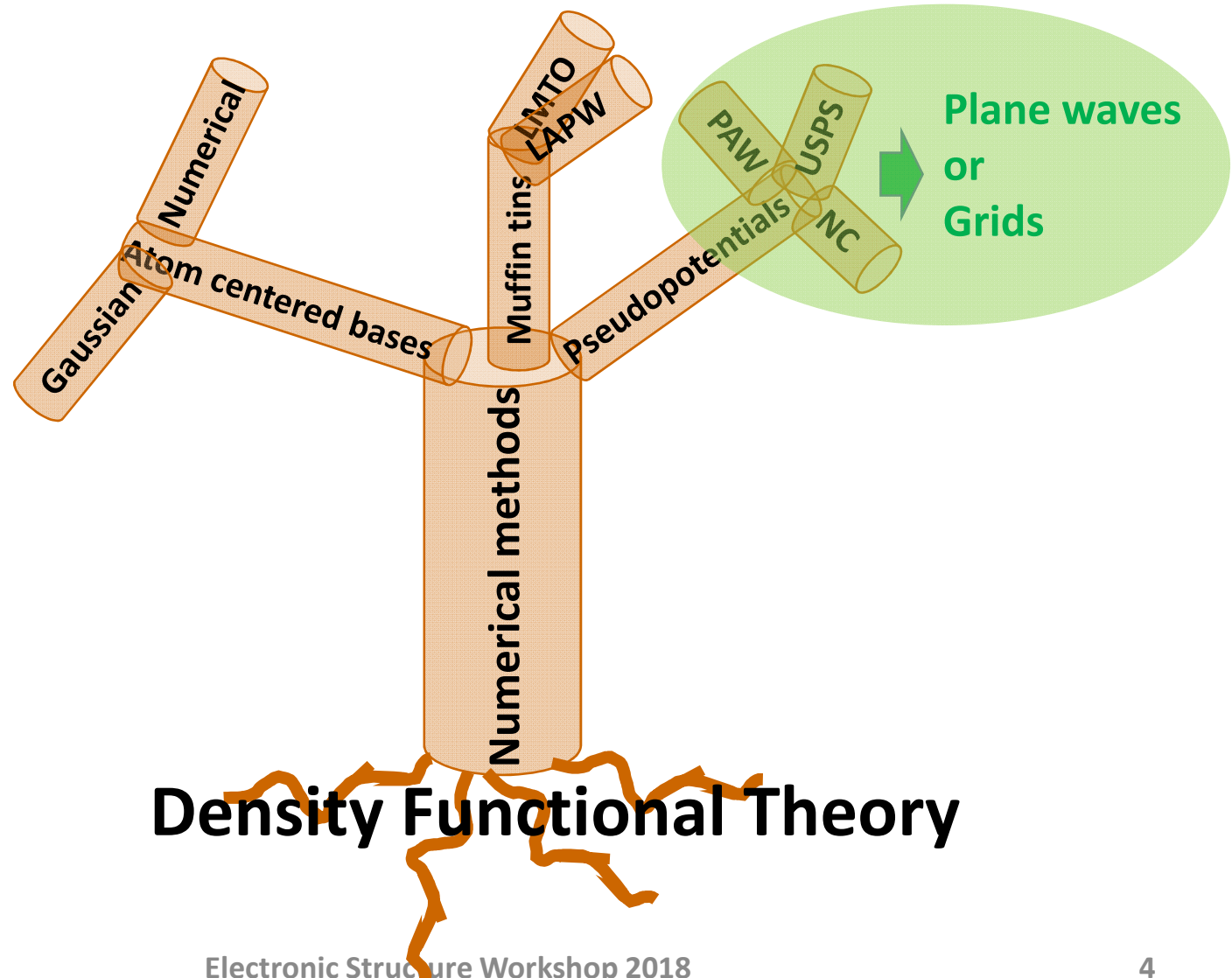
- Cameron Kates, Jamie Drewery, Hannah Zhang, Zachary Pipkorn (former WFU undergrads)
- Zachary Hood (WFU chemistry alum, Ga Tech Ph. D)
- Jason Howard, Ahmad Al-Qawasmeh, Yan Li, Larry E. Rush, Nicholas Lepley (current and former WFU grad students)
- NSF grant DMR-1507942

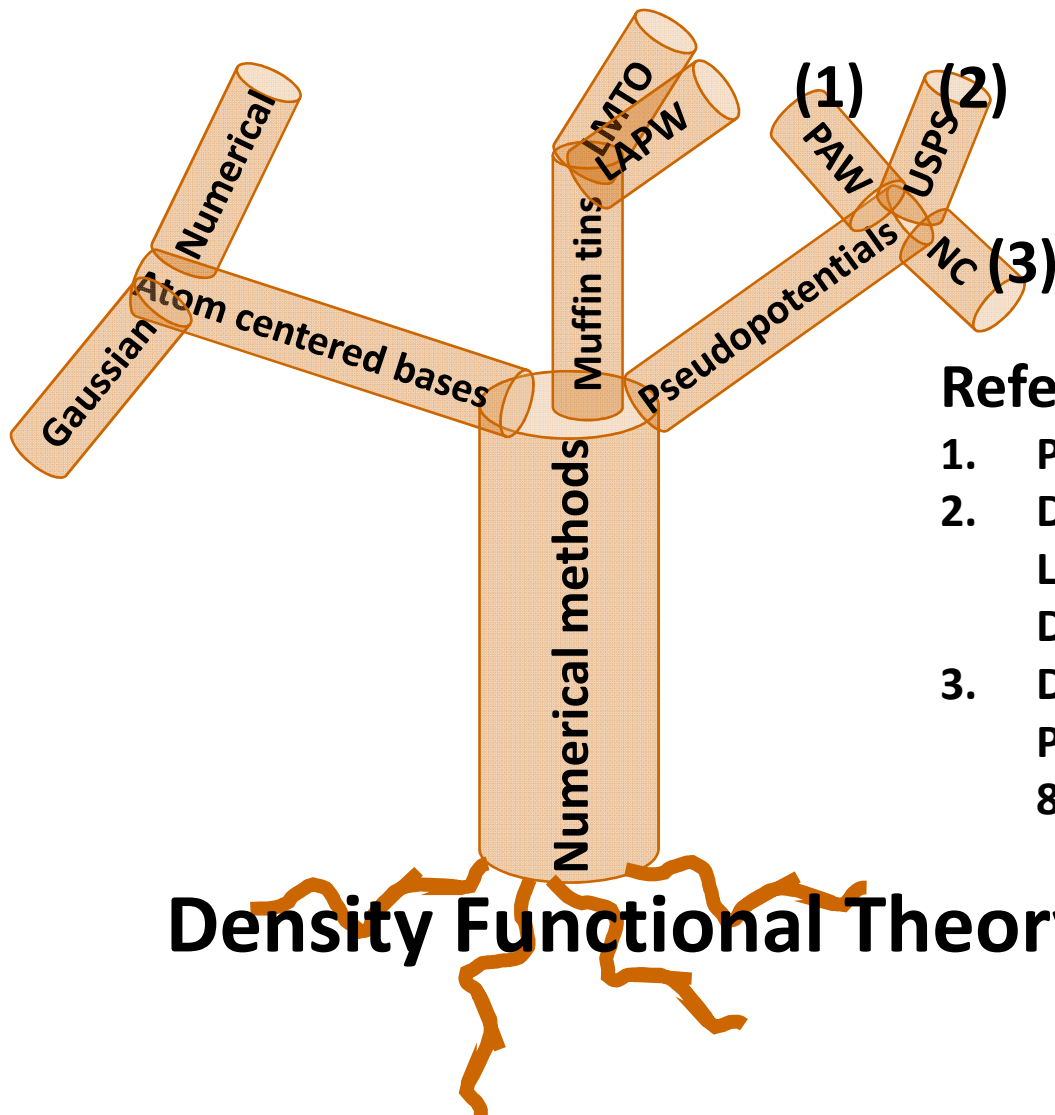
Outline

- **Some history**
- **PAW vs NC and USPP**
- **PAW details**
- **PAW advice**
- **Example application -- the study of solid electrolytes**



Inside the box --





References:

1. P. E. Blöchl, PRB 50, 17953 (1994)
2. D. Vanderbilt, PRB 41, 7892 (1990); K. Laasonen, A. Pasquarello, R. Car, C. Lee, D. Vanderbilt, PRB 47, 10142 (1993)
3. D. R. Hamann, M. Schlüter, C. Chiang, PRL 43, 1494 (1979); D. R. Hamann, PRB 88, 085117 (2013)

Basic ideas of the Projector Augmented Wave (PAW) method



Peter Blöchl,
Institute of Theoretical Physics
TU Clausthal, Germany

Blöchl presented his ideas at ES93 --“PAW: an all-electron method for first-principles molecular dynamics”

Reference: P. E. Blöchl, PRB 50, 17953 (1994)


Features

- Operationally similar to other pseudopotential methods, particularly to the ultra-soft pseudopotential method of D. Vanderbilt; often run within frozen core approximation
- Can retrieve approximate “all-electron” wavefunctions from the results of the calculation; useful for NMR analysis for example
- May have additional accuracy controls particularly of the higher multipole Coulombic contributions.

Basic ideas of the Projector Augmented Wave (PAW) method

- Valence electron wavefunctions are approximated by the form

$$\Psi_{nk}(\mathbf{r}) \approx \tilde{\Psi}_{nk}(\mathbf{r}) + \sum_{ab} \left(\varphi_b^a(\mathbf{r} - \mathbf{R}_a) - \tilde{\varphi}_b^a(\mathbf{r} - \mathbf{R}_a) \right) \langle \tilde{p}_b^a(\mathbf{r} - \mathbf{R}_a) | \tilde{\Psi}_{nk}(\mathbf{r}) \rangle$$


All-electron
wavefunction

Pseudowavefunction,
optimized in solving
Kohn-Sham equations

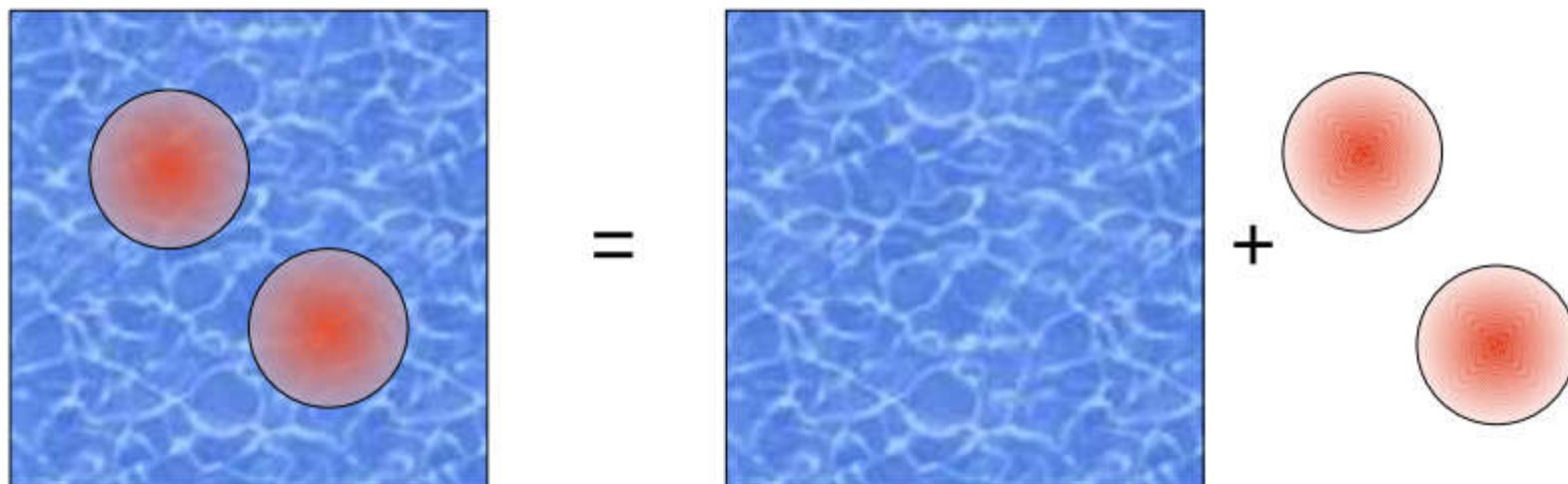
Atom-centered functions:
All electron basis functions
Pseudo basis functions
Projector functions

$\{\tilde{\Psi}_{nk}(\mathbf{r})\}$: determined self-consistently within calculation

$\{\varphi_b^a(\mathbf{r}), \tilde{\varphi}_b^a(\mathbf{r}), \tilde{p}_b^a(\mathbf{r})\}$: part of pseudopotential construction; stored in PAW dataset

Basic ideas of the Projector Augmented Wave (PAW) method

- Evaluation of the total electronic energy:



$$E_{\text{total}} = \tilde{E}_{\text{total}} + \sum_a \Delta E_a$$

Pseudoenergy
(evaluated in plane wave basis or on regular grid)

One-center atomic contributions
(evaluated within augmentation spheres)

Comment on one center energy contributions

- **Norm-conserving pseudopotential scheme using the Kleinman-Bylander method (PRL 48, 1425 (1982)):**
The non-local pseudopotential contributions for site a :

$$\Delta E_a = \sum_{nk,b} W_{nk} \left\langle \tilde{\Psi}_{nk} \left| \tilde{\chi}_b^a \right. \right\rangle \left\langle \tilde{\chi}_b^a \left| \tilde{\Psi}_{nk} \right. \right\rangle, \text{ where } \tilde{\chi}_b^a(\mathbf{r} - \mathbf{R}^a) \text{ are}$$

fixed functions depending on the non-local pseudopotentials and corresponding pseudobasis functions; W_{nk} are occupancy and sampling weights.

- **PAW and USPS :**

$$\Delta E_a = \sum_{nk,bb'} W_{nk} \left\langle \tilde{\Psi}_{nk} \left| \tilde{p}_b^a \right. \right\rangle M_{bb'}^a \left\langle \tilde{p}_{b'}^a \left| \tilde{\Psi}_{nk} \right. \right\rangle, \text{ where } \tilde{p}_b^a(\mathbf{r} - \mathbf{R}^a) \text{ are}$$

projector functions, $M_{bb'}^a$ are matrix elements depending on all-electron and pseudobasis functions, and W_{nk} are occupancy and Brillouin zone sampling weights.

Comment on one center energy contributions

-- continued for PAW and USPS



$M_{bb'}^a$ matrix elements (different for USPS and PAW) are evaluated within the augmentation spheres. For example, the kinetic energy term:

$$K_{bb'}^a = \delta_{l_b l_{b'}} \delta_{m_b m_{b'}} \frac{\hbar^2}{2m} \left(\int_0^{r_c} dr \left(\frac{d\phi_b^a(r)}{dr} \frac{d\phi_{b'}^a(r)}{dr} - \frac{d\tilde{\phi}_b^a(r)}{dr} \frac{d\tilde{\phi}_{b'}^a(r)}{dr} \right) + l_b(l_b + 1) \left(\int_0^{r_c} \frac{dr}{r^2} \left(\phi_b^a(r) \phi_{b'}^a(r) - \tilde{\phi}_b^a(r) \tilde{\phi}_{b'}^a(r) \right) \right) \right)$$

$$\text{where } \phi_b^a(\mathbf{r}) \equiv \frac{\phi_b^a(r)}{r} Y_{l_b m_b}(\hat{\mathbf{r}}) \text{ and } \tilde{\phi}_b^a(\mathbf{r}) \equiv \frac{\tilde{\phi}_b^a(r)}{r} Y_{l_b m_b}(\hat{\mathbf{r}})$$

Note that for USPS, the operator $Q_{bb'}^a(r) \equiv \left(\phi_b^a(r) \phi_{b'}^a(r) - \tilde{\phi}_b^a(r) \tilde{\phi}_{b'}^a(r) \right)$ is pseudized, while for PAW it is evaluated within matrix elements and "compensation charges" are added. In both cases, multipole moments are conserved.

Summary of properties of norm-conserving (NC), ultra-soft-pseudopotential (USPS) and projector augmented wave (PAW) methods

	NC	USPS	PAW
Conservation of charge	✓	✓	✓
Multipole moments in Hartree interaction		✓	✓
Retrieve all-electron wavefunction			✓

Some details – use of “compensation charge”

PAW approximation to valence all-electron wave function

$$\Psi_{nk}(\mathbf{r}) \approx \tilde{\Psi}_{nk}(\mathbf{r}) + \sum_{ab} \left(\varphi_b^a(\mathbf{r} - \mathbf{R}_a) - \tilde{\varphi}_b^a(\mathbf{r} - \mathbf{R}_a) \right) \langle \tilde{p}_b^a(\mathbf{r} - \mathbf{R}_a) | \tilde{\Psi}_{nk}(\mathbf{r}) \rangle$$

PAW approximation to all-electron density

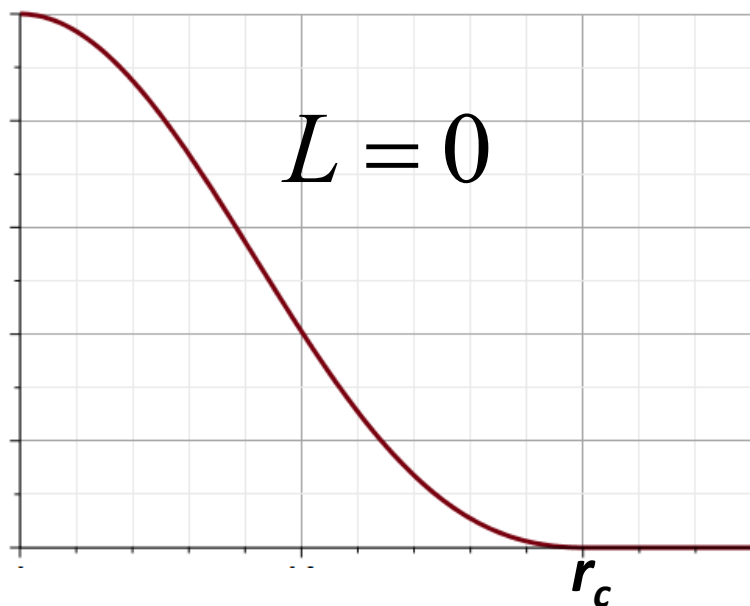
$$\begin{aligned} n_{\text{valence}}(\mathbf{r}) &\approx \sum_{nk} W_{nk} |\Psi_{nk}(\mathbf{r})|^2 \\ &\approx \sum_{nk} W_{nk} |\tilde{\Psi}_{nk}(\mathbf{r})|^2 \\ &+ \sum_{nk} W_{nk} \sum_{a,bb'} \langle \tilde{\Psi}_{nk} | \tilde{p}_b^a \rangle \langle \tilde{p}_{b'}^a | \tilde{\Psi}_{nk} \rangle \left(\varphi_b^a(\mathbf{r} - \mathbf{R}_a) \varphi_{b'}^a(\mathbf{r} - \mathbf{R}_a) - \tilde{\varphi}_b^a(\mathbf{r} - \mathbf{R}_a) \tilde{\varphi}_{b'}^a(\mathbf{r} - \mathbf{R}_a) \right) \\ &\equiv \sum_{nk} W_{nk} \left(|\tilde{\Psi}_{nk}(\mathbf{r})|^2 + \sum_{a,bb'} \langle \tilde{\Psi}_{nk} | \tilde{p}_b^a \rangle \langle \tilde{p}_{b'}^a | \tilde{\Psi}_{nk} \rangle Q_{bb'}^a(\mathbf{r} - \mathbf{R}_a) \right) \\ &\equiv \tilde{n}(\mathbf{r}) + \sum_a \left(n^a(\mathbf{r} - \mathbf{R}_a) - \tilde{n}^a(\mathbf{r} - \mathbf{R}_a) \right) \\ &= \tilde{n}(\mathbf{r}) + \sum_a \hat{n}^a(\mathbf{r} - \mathbf{R}^a) + \sum_a \left(n^a(\mathbf{r} - \mathbf{R}_a) - \tilde{n}^a(\mathbf{r} - \mathbf{R}_a) - \hat{n}^a(\mathbf{r} - \mathbf{R}^a) \right) \end{aligned}$$

Some details – use of “compensation charge” -- continued

Compensation charge is designed to have the same multipole moments of one-center charge differences:

$$\int_{r \leq r_c^a} d^3 r r^L Y_{LM}(\hat{\mathbf{r}}) \hat{n}^a(\mathbf{r}) = \int_{r \leq r_c} d^3 r r^L Y_{LM}(\hat{\mathbf{r}}) (n^a(\mathbf{r}) - \tilde{n}^a(\mathbf{r}))$$

Typical shape of
compensation charge
for L=0 component --



Some details – use of “compensation charge” -- continued


The inclusion of the "compensation" charge ensures

1. Hartree energy of smooth charge density represents correct charge
2. Hartree energy contributions of one-center charge is confined within augmentation sphere:

$$\int_{r \leq r_c^a} d^3 r' \frac{n^a(\mathbf{r}) - \tilde{n}^a(\mathbf{r}) - \hat{n}^a(\mathbf{r})}{|\mathbf{r} - \mathbf{r}'|} = \begin{cases} V_{\text{Hartree}}^a(\mathbf{r}) & \text{for } r \leq r_c^a \\ 0 & \text{for } r > r_c^a \end{cases}$$

Some details – form of exchange-correlation contributions

For $E_{xc}[n(\mathbf{r})] \equiv \int d^3r K_{xc}(n(\mathbf{r})):$

 non-linear core correction (S. G. Louie et al. PRB 26, 1738 (1982))

Smooth contribution: $\tilde{E}_{xc} = E_{xc}[\tilde{n}(\mathbf{r}) + \tilde{n}_{\text{core}}(\mathbf{r})]$

One-center contributions: $E_{xc}^a - \tilde{E}_{xc}^a = E_{xc}[n^a(\mathbf{r}) + n_{\text{core}}^a(\mathbf{r})] - E_{xc}[\tilde{n}^a(\mathbf{r}) + \tilde{n}_{\text{core}}^a(\mathbf{r})]$

Note that VASP and Quantum-Espresso use

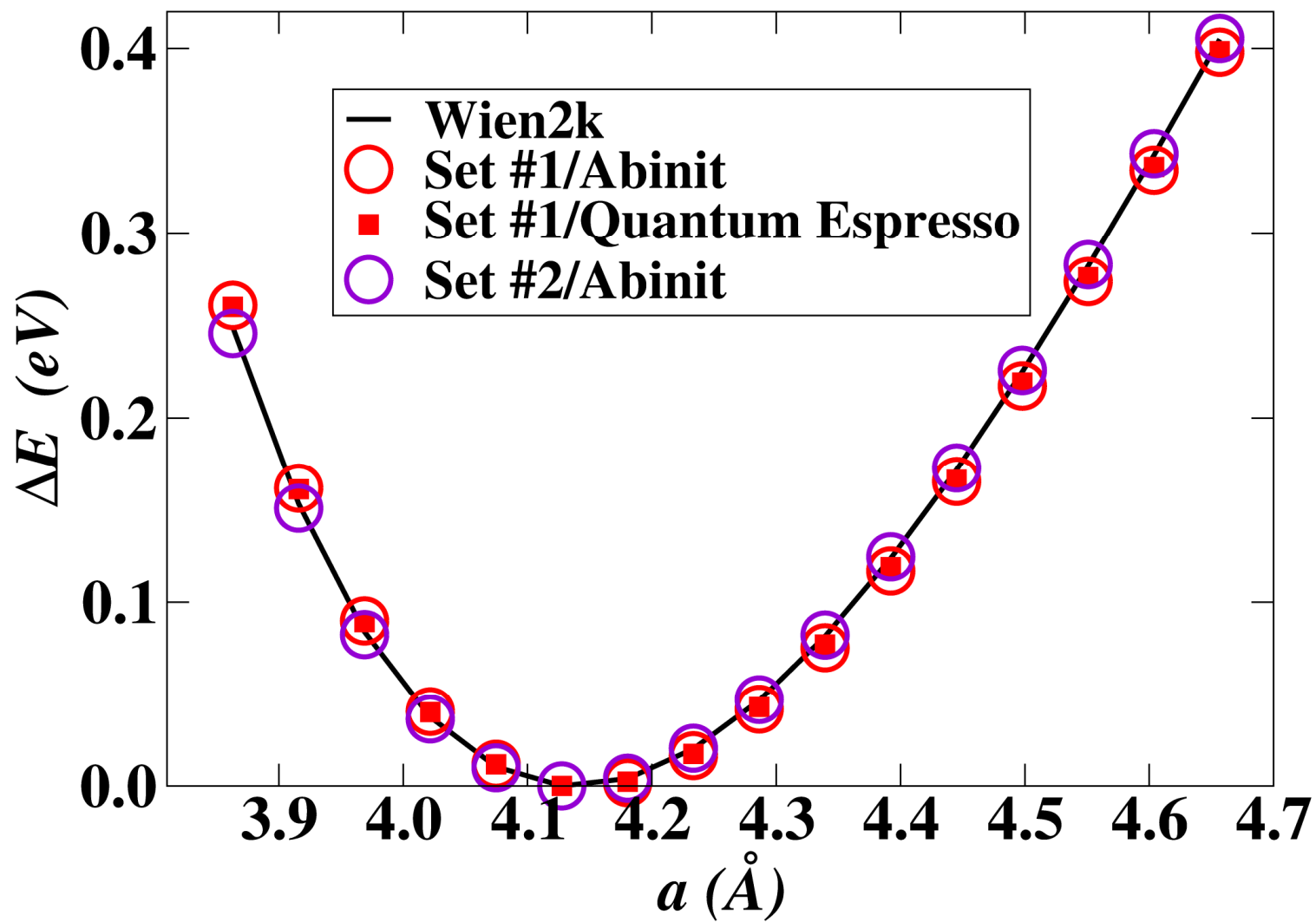
$$E_{xc}[\tilde{n}(\mathbf{r}) + \tilde{n}_{\text{core}}(\mathbf{r}) + \hat{n}(\mathbf{r})]$$

and $E_{xc}[\tilde{n}^a(\mathbf{r}) + \tilde{n}_{\text{core}}^a(\mathbf{r}) + \hat{n}^a(\mathbf{r})]$

which can cause trouble occasionally.

Measure of accuracy

Binding energy curve for CsBr



Recipes for constructing projector and basis functions

$$\varphi_b^a(\mathbf{r}) = \frac{\varphi_b^a(r)}{r} Y_{l_b m_b}(\hat{\mathbf{r}}) \quad \tilde{\varphi}_b^a(\mathbf{r}) = \frac{\tilde{\varphi}_b^a(r)}{r} Y_{l_b m_b}(\hat{\mathbf{r}}) \quad \tilde{p}_b^a(\mathbf{r}) = \frac{\tilde{p}_b^a(r)}{r} Y_{l_b m_b}(\hat{\mathbf{r}})$$

Constraints: $\tilde{\varphi}_b^a(r) = \varphi_b^a(r)$ for $r \geq r_c^a$

$\tilde{p}_b^a(r) = 0$ for $r \geq r_c^a$

$$\langle \tilde{p}_b^a | \tilde{\varphi}_{b'}^a \rangle = \delta_{bb'}$$

Peter Blöchl's scheme (set #1)

Choose projectors $\tilde{p}_b^a(r)^*$

\Rightarrow Derive $\tilde{\varphi}_b^a(r)$

***Typically Bessel-like function with zero value and derivative at r_c^a**

David Vanderbilt's scheme (set #2)

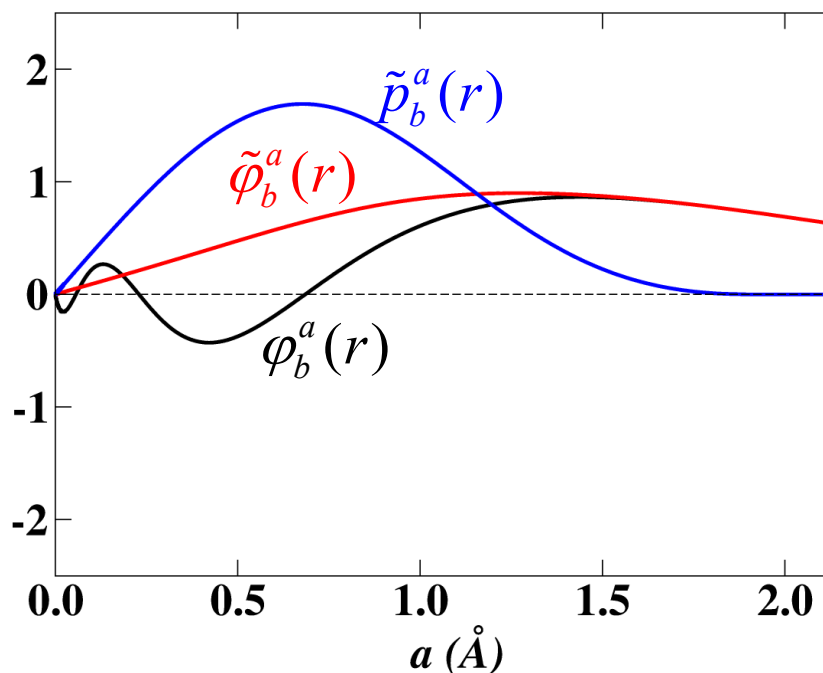
Choose pseudo bases $\tilde{\varphi}_b^a(r)^*$

\Rightarrow Derive $\tilde{p}_b^a(r)$

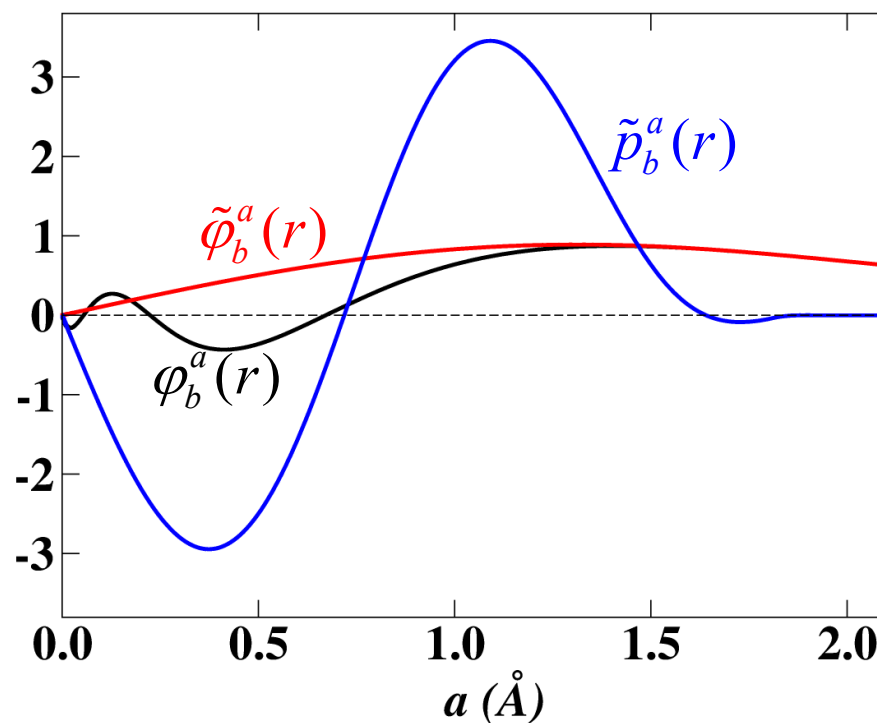
***Polynomial or Bessel function form following RRKJ, PRB 41, 1227 (1990)**

Example projector and basis functions

Br 4s orbital



From set #1

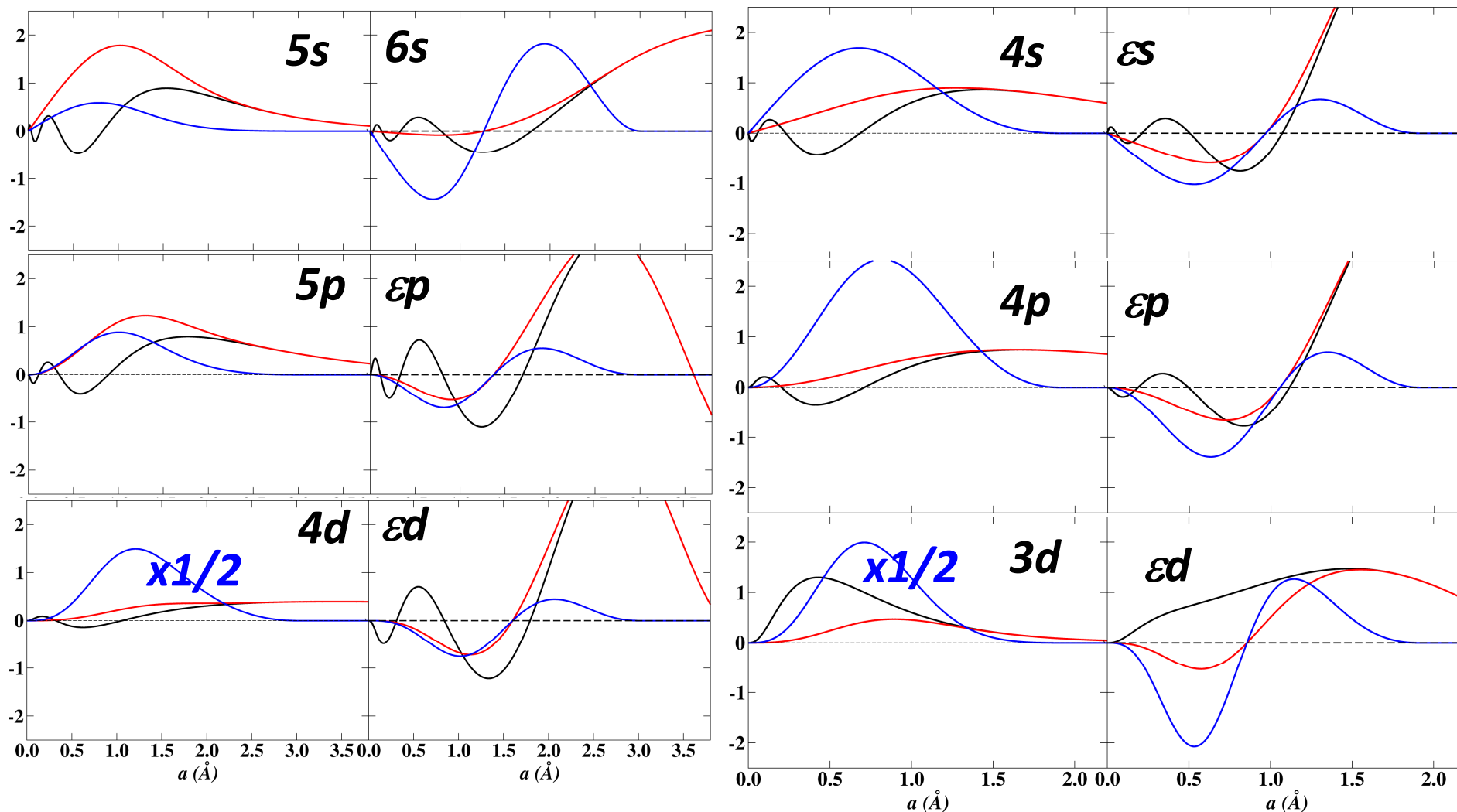


From set #2

Set of basis and projector functions for set #1

Cs

Br



Efforts to use machine learning methods to optimize PAW datasets

Computer Physics Communications 196 (2015) 267–275



ELSEVIER

Contents lists available at [ScienceDirect](#)

Computer Physics Communications

journal homepage: www.elsevier.com/locate/cpc



Automated generation of highly accurate, efficient and transferable pseudopotentials



R.A. Hansel^a, C.N. Brock^a, B.C. Paikoff^b, A.R. Tackett^c, D.G. Walker^{b,*}

^a Materials Science Program, Vanderbilt University, United States

^b Department of Mechanical Engineering, Vanderbilt University, United States

^c Department of Astronomy and Physics, Vanderbilt University, United States

[Journal of Computational Physics 347 \(2017\) 39–55](#)

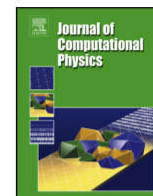


ELSEVIER

Contents lists available at [ScienceDirect](#)

Journal of Computational Physics

www.elsevier.com/locate/jcp



Evolutionary optimization of PAW data-sets for accurate high pressure simulations



Kanchan Sarkar^{a,*}, Mehmet Topsakal^a, N.A.W. Holzwarth^b,
Renata M. Wentzcovitch^{a,c}

^a Department of Chemical Engineering and Materials Science, University of Minnesota, Minneapolis, MN 55455, USA

^b Department of Physics, Wake Forest University, Winston-Salem, NC 27109, USA

^c Minnesota Supercomputing Institute for Digital Technology and Advanced Computations, University of Minnesota, Minneapolis, MN 55455, USA

General advice about generating PAW datasets

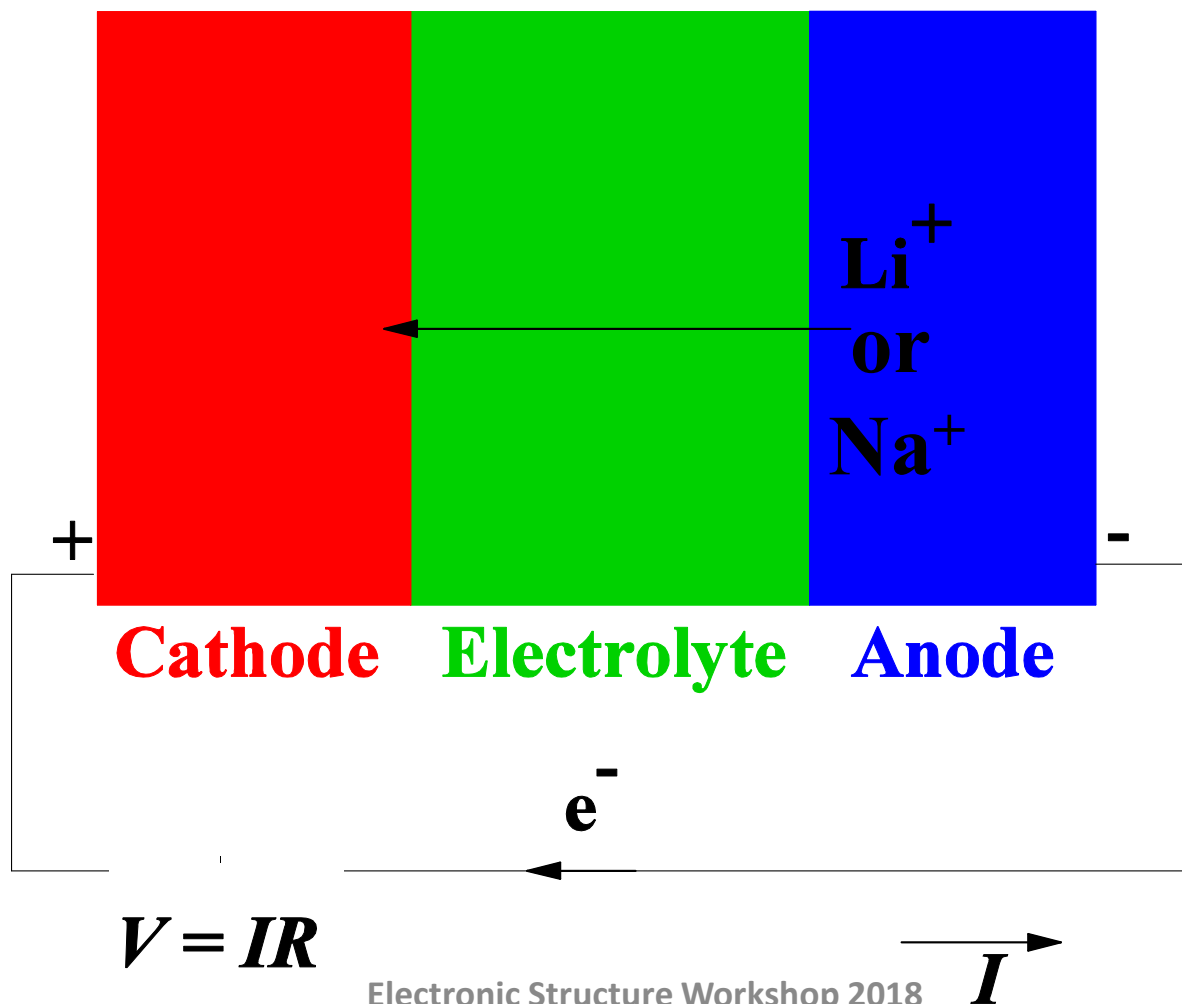


- **ATOMPAW code*** available at <http://pwpaw.wfu.edu>
- **Develop and test atomic datasets for the full scope of your project** → determines r_c^a .
- **Determine local pseudopotential from self-consistent all-electron potential**
- **Determine basis functions, with or without semicore states; usually 2 sets of basis functions and projectors for each / channel.**
- **Test binding energy curves for a few binary compounds related to your project.**
- **Check plane wave (or grid spacing convergence of your data sets before starting production runs.**

***With major modification by Marc Torrent and other Abinit developers.**

Simulations of Idealized Solid Electrolytes

Theoretical battery



What can first principles modeling bring to the development of all solid state batteries?

- **Examine structures and stabilities of potential ionic conductors**
- **Examine mechanisms and model efficiencies for ionic conduction**
- **Model ideal interfaces between electrolytes and electrodes**

From Oak Ridge National Laboratory:



Materials
Views

www.MaterialsViews.com

Adv. Energy Mater. 2015, 5, 1401408

DOI: 10.1002/aenm.201401408

ADVANCED
ENERGY
MATERIALS

www.advenegymat.de

Solid Electrolyte: the Key for High-Voltage Lithium Batteries

Juchuan Li,* Cheng Ma, Miaofang Chi, Chengdu Liang, and Nancy J. Dudney*

Advantages

- Compatible and stable with high voltage cathodes and with Li metal anodes

Disadvantages

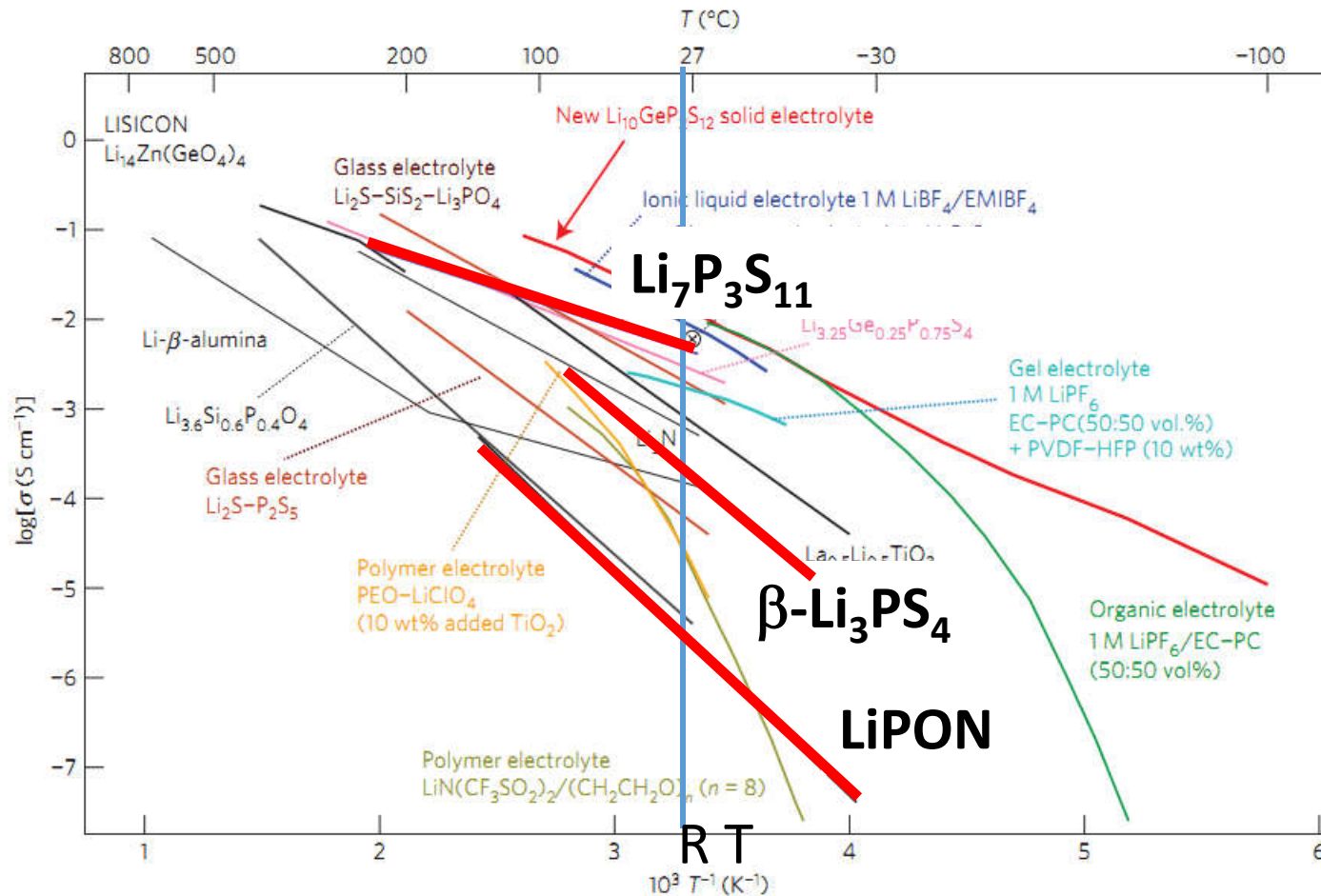
- Relatively low ionic conductivity (Compensated with the use of less electrolyte?)
- Lower total capacity

Demonstrated for $\text{LiNi}_{0.5}\text{Mn}_{1.5}\text{O}_4/\text{LiPON}/\text{Li}$

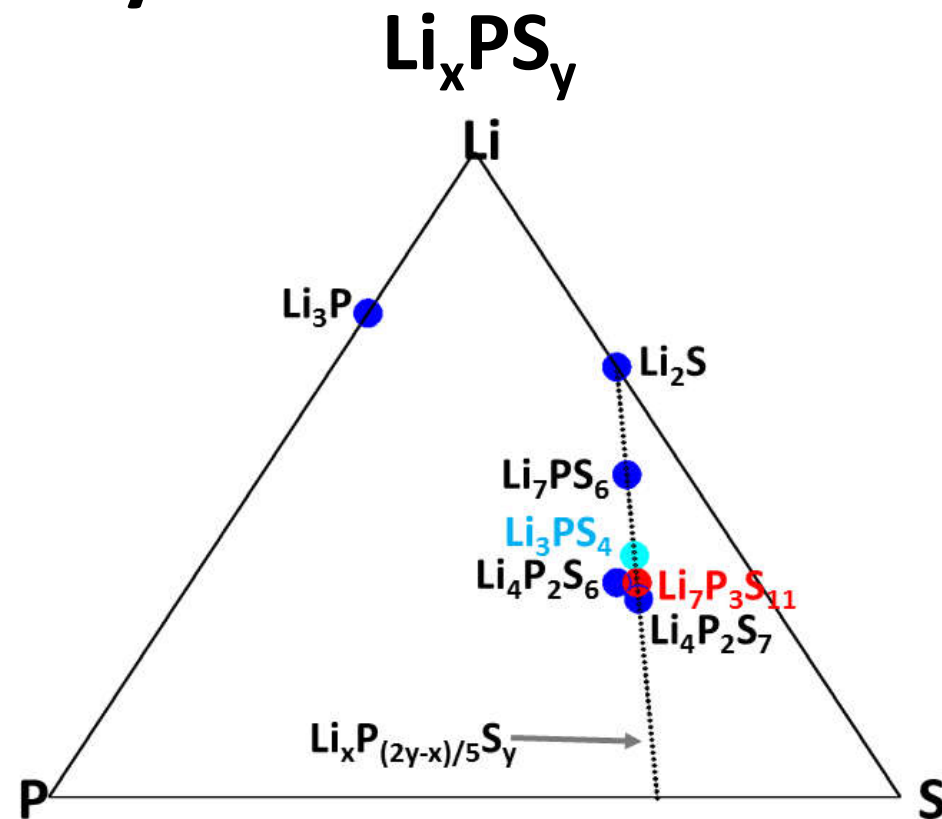
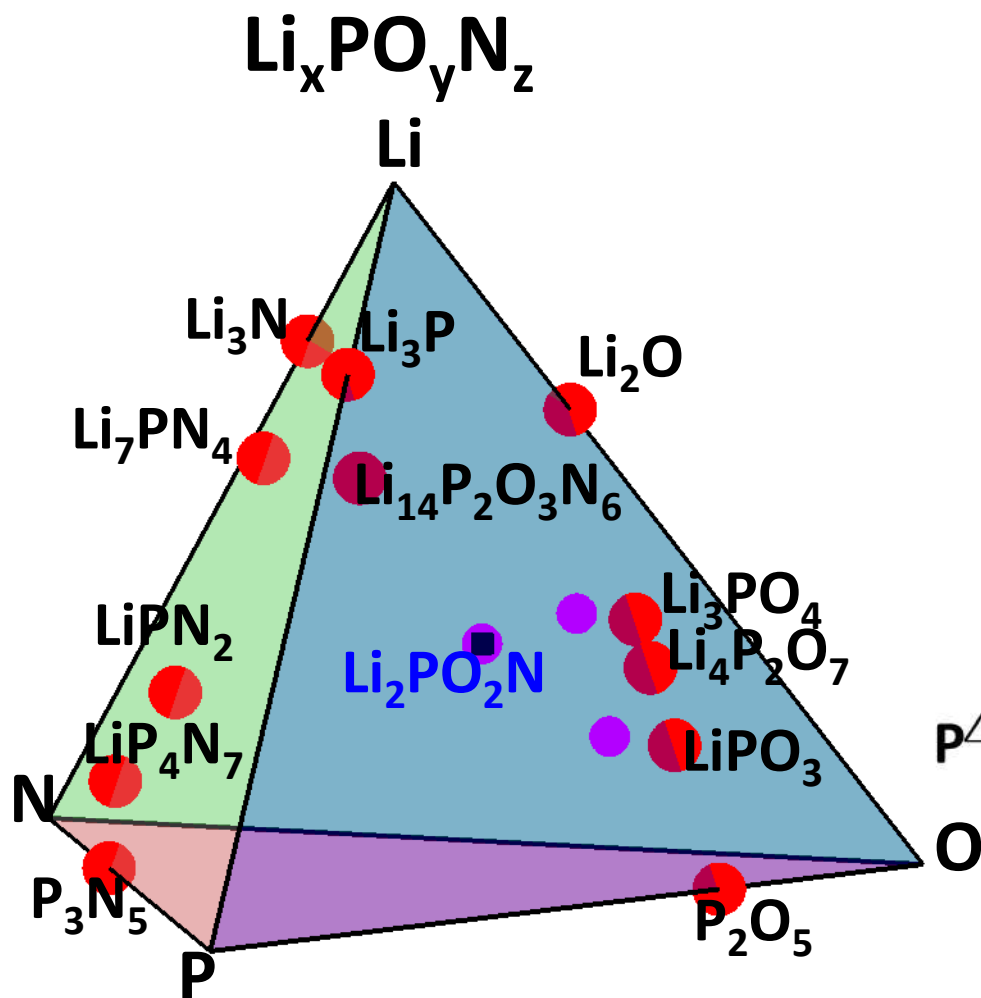
- 10^{-6} m LiPON electrolyte layer achieved adequate conductivity
- 10,000 cycles* with 90% capacity retention

*1 cycle per day for 27 years

Motivation: Paper by N. Kamaya, *et. al* in *Nature Materials* 10, 682-686 (2011)



Solid electrolyte families investigated in this study:








+ a few related materials such as Li_4SnS_4 , $\text{Na}_4\text{P}_2\text{S}_6$, Na_3SbS_4

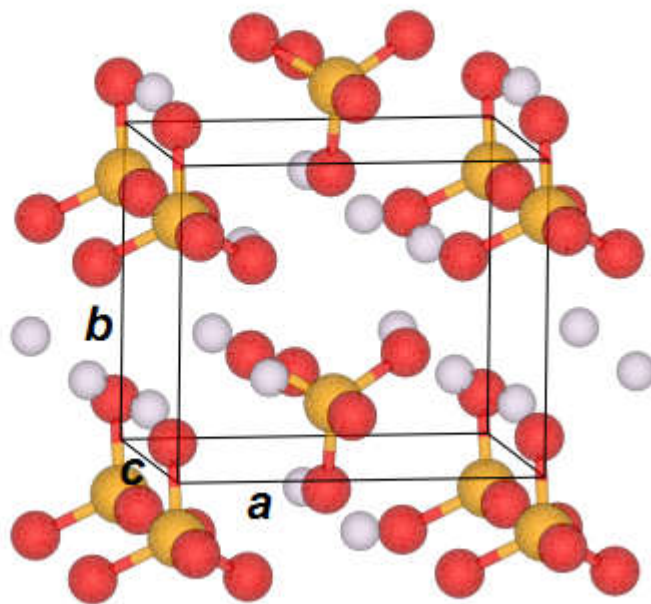
Li₃PO₄ crystals

γ -Li₃PO₄

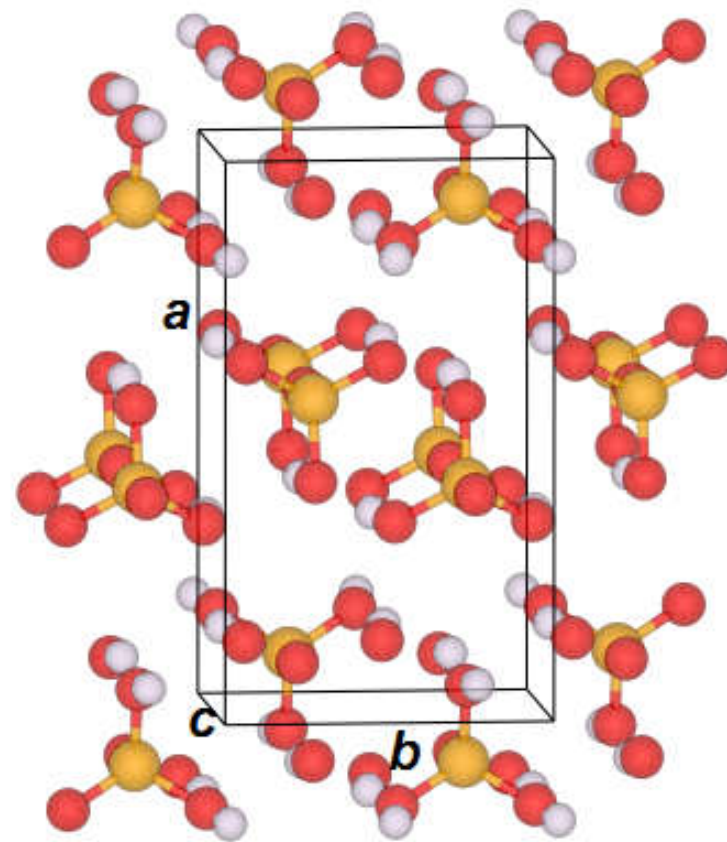
Key

-  Li
-  N
-  O
-  P
-  S

β -Li₃PO₄



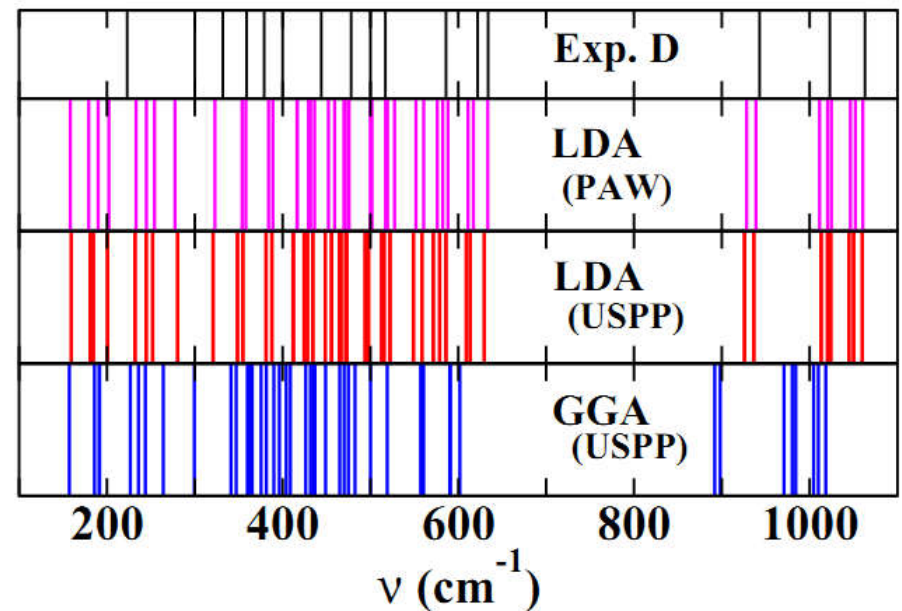
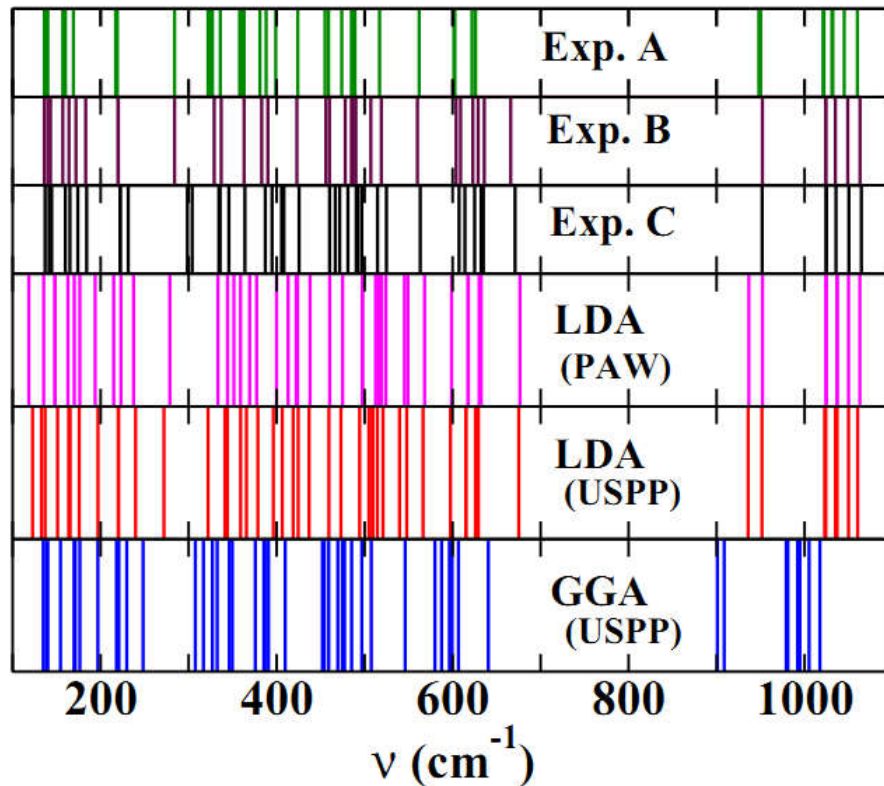
(*Pmn2*₁)



(*Pnma*)

Validation of calculations

Raman spectra – Experiment & Calculation



A: B. N. Mavrin et al, J. Exp. Theor. Phys. **96**,53 (2003); B: F. Harbach and F. Fischer, Phys. Status Solidi B **66**, 237 (1974) – room temp. C: Ref. B at liquid nitrogen temp.; D: L. Popović et al, J. Raman Spectrosc. **34**,77 (2003).

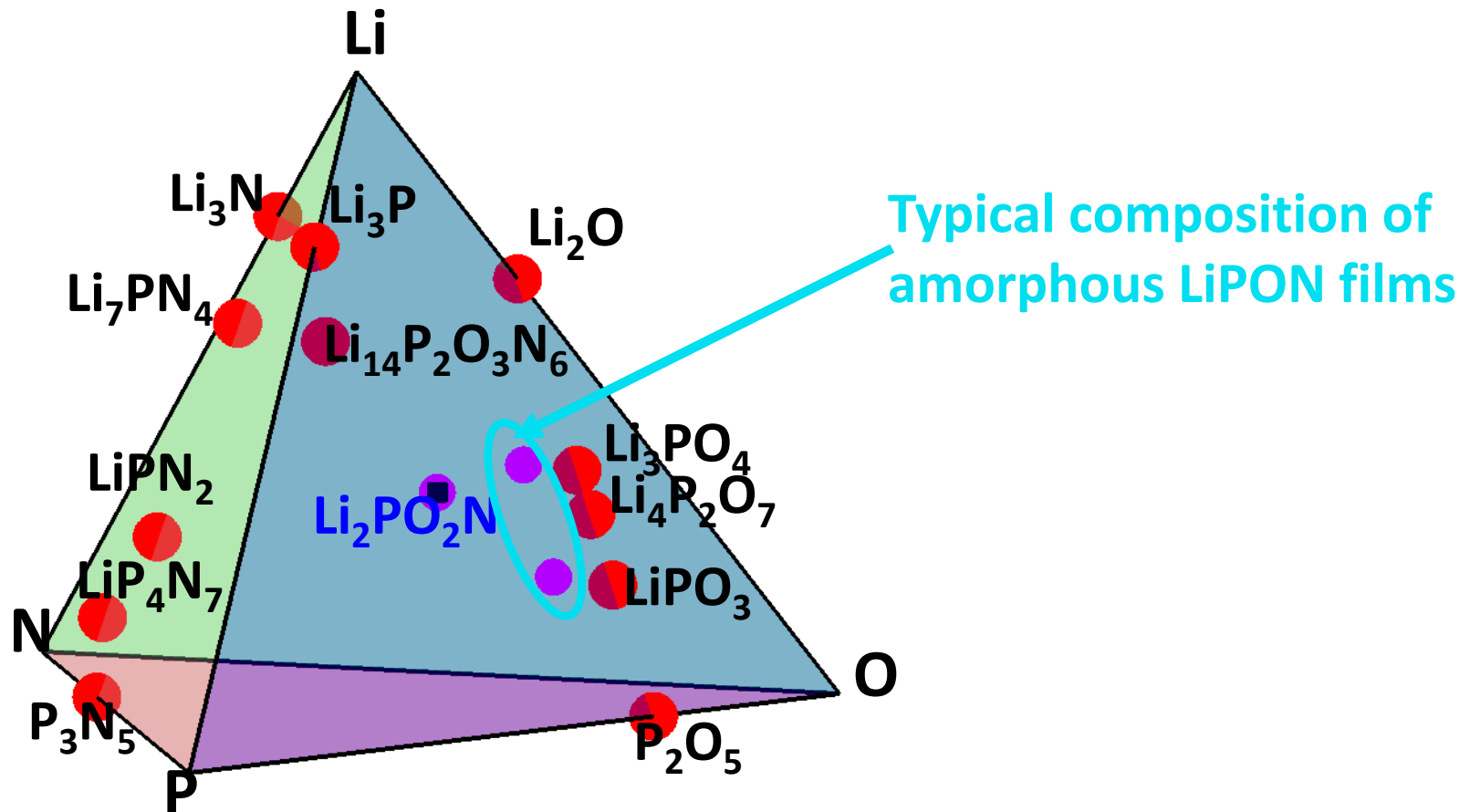
Heats of formation – Experiment & Calculation



Table 1. Calculated heats of formation for Li phosphates, phospho-nitrides, related materials. The structural designation uses the the notation defined in the International Tables of Crystallography⁸⁵ based on structural information reported in the International Crystal Structure Database.⁸⁶ The heats of formation ΔH (eV/FU) are given in units of eV per formula unit. When available from Ref. [31] and [32] experiment values are indicated in parentheses. Those indicated with “*” were used fitting the O and N reference energies as explained in the text.

Material	Structure	ΔH (eV/FU)	Material	Structure	ΔH (eV/FU)
β -Li ₃ PO ₄	<i>Pmn</i> 2 ₁ (#31)	-21.23	N ₂ O ₅	<i>P6</i> ₃ / <i>mmc</i> (#194)	- 0.94 (- 0.45*)
γ -Li ₃ PO ₄	<i>Pnma</i> (#62)	-21.20 (-21.72*)	P ₃ N ₅	<i>C2/c</i> (#15)	- 3.02 (- 3.32*)
γ -Li ₃ PS ₄	<i>Pmn</i> 2 ₁ (#31)	- 8.37	<i>h</i> -P ₂ O ₅	<i>R3c</i> (#161)	-15.45 (-15.53*)
β -Li ₃ PS ₄	<i>Pnma</i> (#62)	- 8.28	α -P ₂ O ₅	<i>Fdd</i> 2 (#43)	-15.78
Li ₄ P ₂ O ₆	<i>P</i> $\bar{3}$ 1 <i>m</i> (#162)	-29.72	P ₂ S ₅	<i>P</i> $\bar{1}$ (#2)	- 1.93
Li ₄ P ₂ O ₇	<i>P</i> $\bar{1}$ (#2)	-33.97	P ₄ S ₃	<i>Pnma</i> (#62)	- 2.45 (- 2.33)
Li ₅ P ₂ O ₆ N	<i>P</i> $\bar{1}$ (#2)	-33.18	SO ₃	<i>Pna</i> 2 ₁ (#33)	- 4.84 (- 4.71*)
Li ₄ P ₂ S ₆	<i>P</i> $\bar{3}$ 1 <i>m</i> (#162)	-12.42	Li ₃ N	<i>P6/mmm</i> (#191)	- 1.60 (- 1.71*)
Li ₄ P ₂ S ₇	<i>P</i> $\bar{1}$ (#2)	-11.59	Li ₂ O	<i>Fm</i> $\bar{3}$ <i>m</i> (#225)	- 6.10 (- 6.20*)
Li ₇ P ₃ O ₁₁	<i>P</i> $\bar{1}$ (#2)	-54.84	Li ₂ O ₂	<i>P6</i> ₃ / <i>mmc</i> (#194)	- 6.35 (- 6.57*)
Li ₇ P ₃ S ₁₁	<i>P</i> $\bar{1}$ (#2)	-20.01	Li ₃ P	<i>P6</i> ₃ / <i>mmc</i> (#194)	- 3.47
LiPO ₃	<i>P2/c</i> (#13)	-12.75	Li ₂ S	<i>Fm</i> $\bar{3}$ <i>m</i> (#225)	- 4.30 (- 4.57)
LiPN ₂	<i>I</i> $\bar{4}$ 2 <i>d</i> (#122)	- 3.65	Li ₂ S ₂	<i>P6</i> ₃ / <i>mmc</i> (#194)	- 4.09
<i>s1</i> -Li ₂ PO ₂ N	<i>Pbcm</i> (#57)	-12.35	LiNO ₃	<i>R</i> $\bar{3}$ <i>c</i> (#167)	- 5.37 (- 5.01*)
<i>SD</i> -Li ₂ PO ₂ N	<i>Cmc</i> 2 ₁ (#36)	-12.47	Li ₂ SO ₄	<i>P2</i> ₁ / <i>c</i> (#14)	-14.63 (-14.89*)
<i>SD</i> -Li ₂ PS ₂ N	<i>Cmc</i> 2 ₁ (#36)	- 5.80			

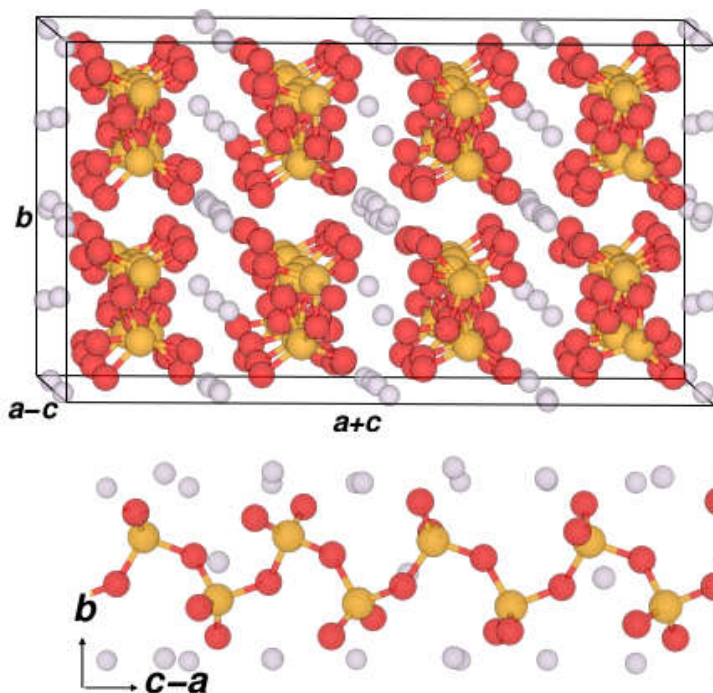
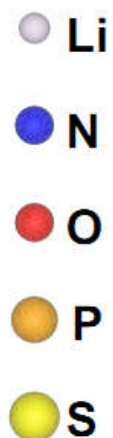
**Systematic study of LiPON materials – $\text{Li}_x\text{PO}_y\text{N}_z$ –
(Yaojun A. Du and N. A. W. Holzwarth, Phys. Rev. B 81, 184106 (2010))**



Experimentally known structure



Key



Computationally predicted structure

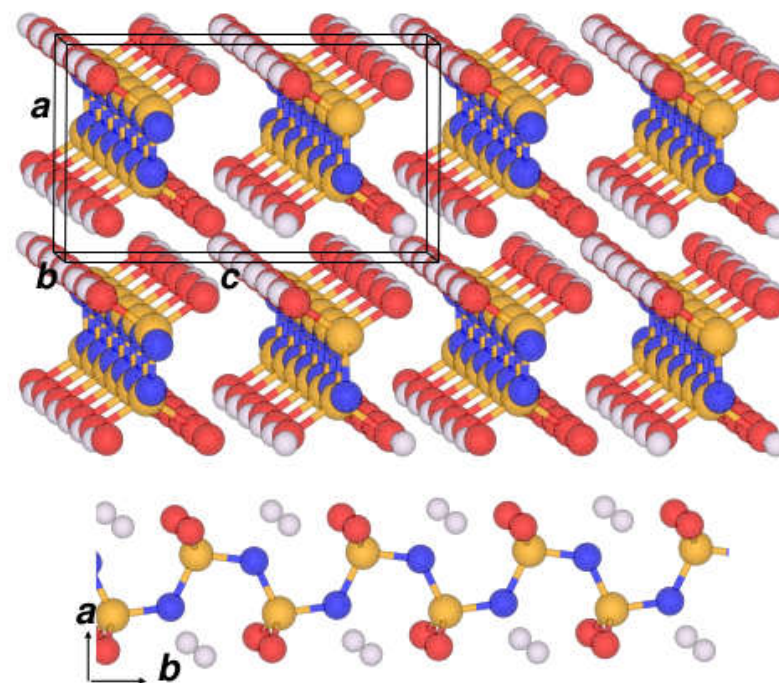
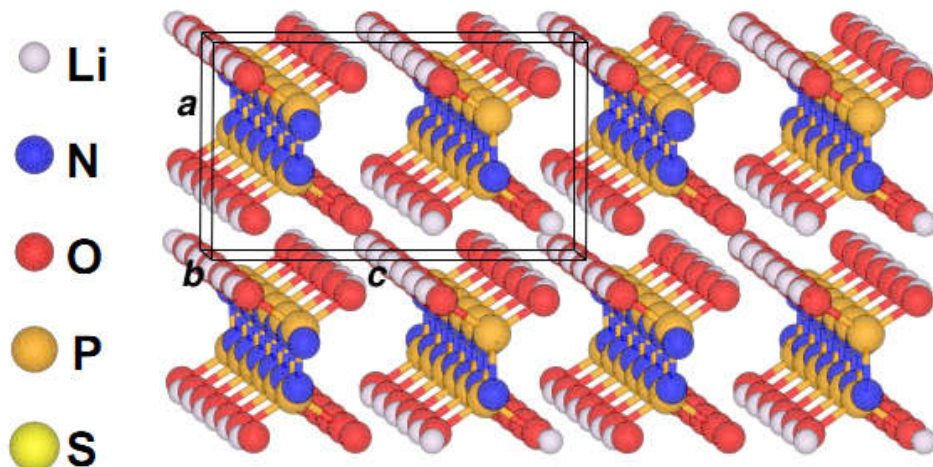


Fig. 7. Ball and stick diagrams for LiPO_3 in the $P2/c$ structure (20 formula units per unit cell) and $s_1\text{-Li}_2\text{PO}_2\text{N}$ in the $Pbcm$ structure (4 formula units per unit cell) from the calculated results. For each crystal diagram, a view of a horizontal chain axis is also provided for a single phosphate or phospho-nitride chain.

Computationally predicted structure

Key

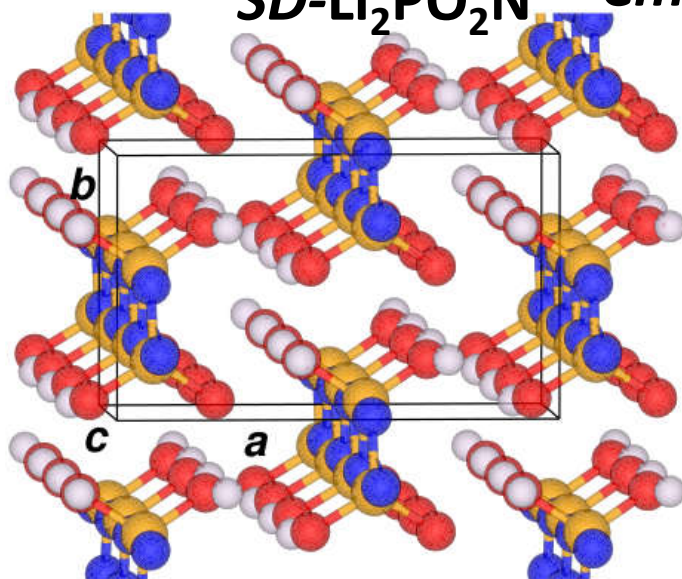
s_1 -Li₂PO₂N *Pbcm*



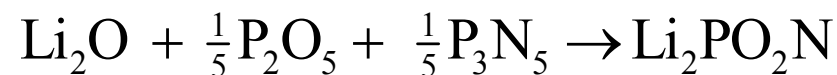
Calculations have now verified that the *SD* structure is more stable than the s_1 structure by 0.1 eV/FU.

Experimentally realized structure

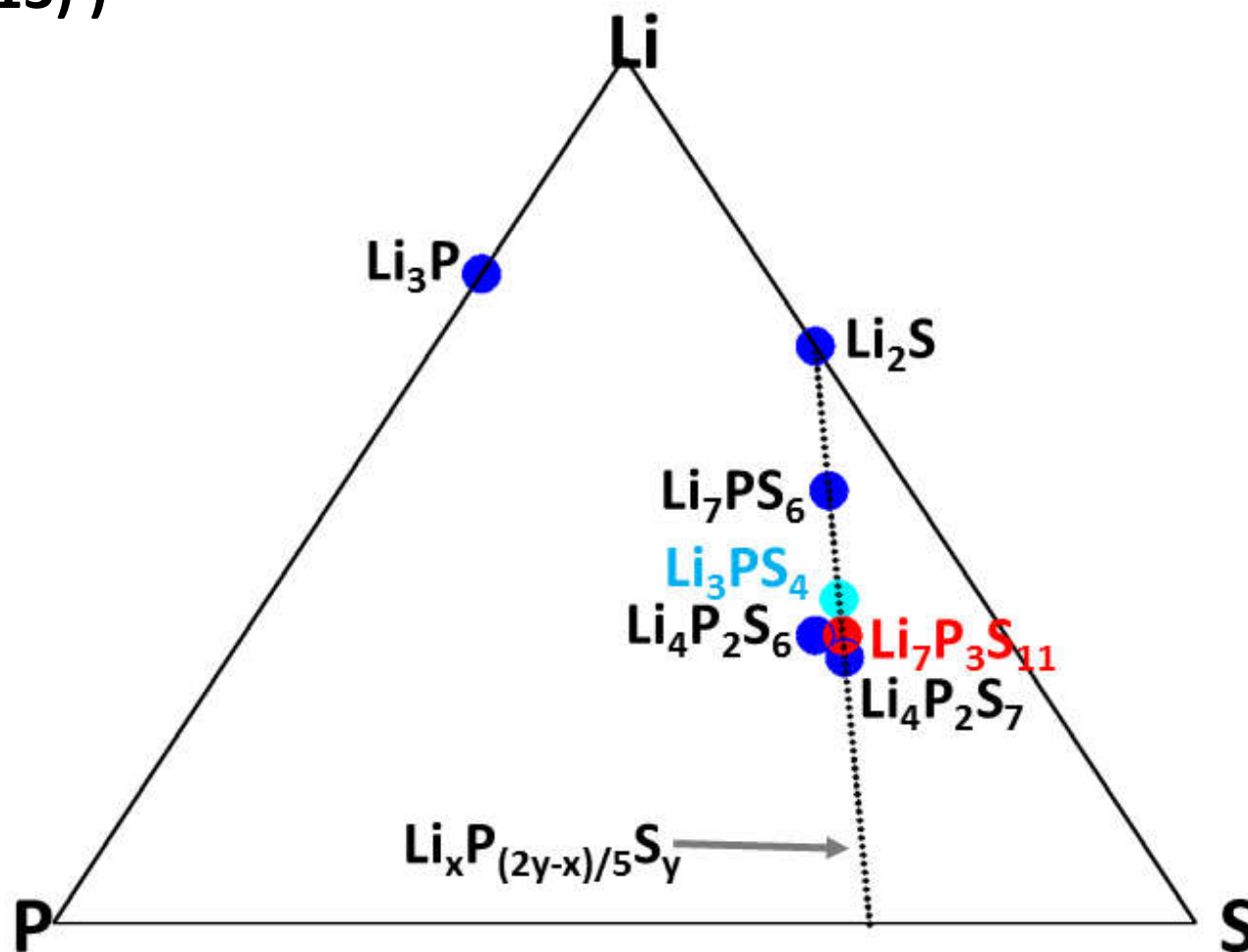
SD-Li₂PO₂N *Cmc2₁*



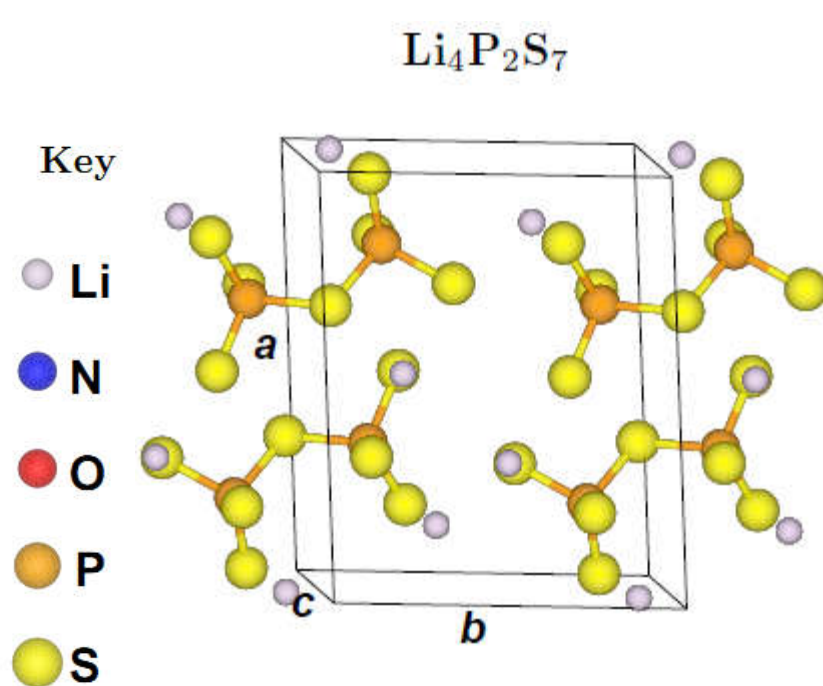
Synthesis of Li₂PO₂N by Keerthi Senevirathne, Cynthia Day, Michael Gross, and Abdessadek Lachgar (SSI 233, 95-101 (2013))
High temperature solid state synthesis using reaction:



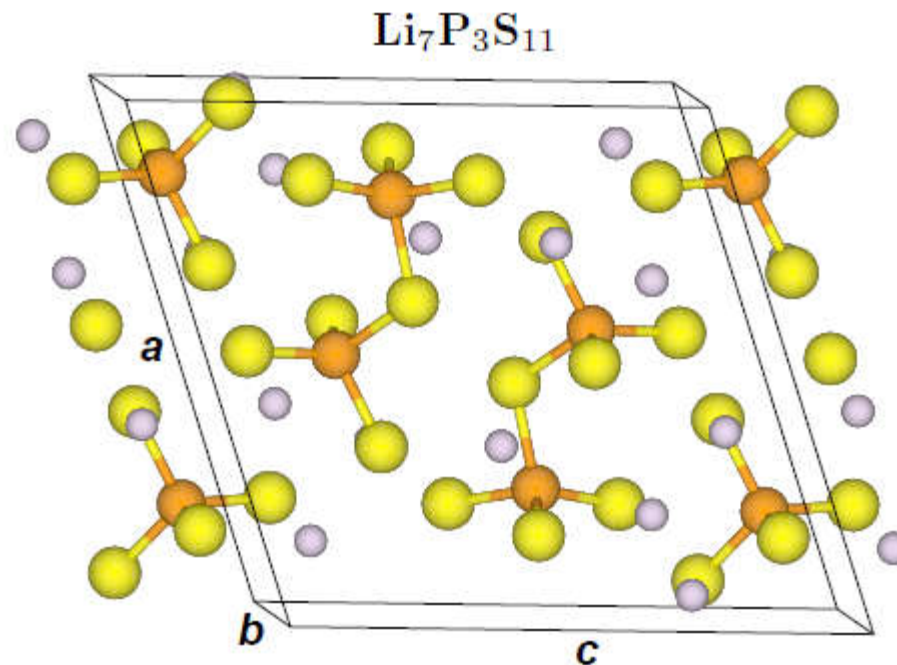
Systematic study of Li_xPS_y materials – (N. D. Lepley and N. A. W. Holzwarth, J. Electrochem. Soc. 159, A538 (2012), Phys. Rev. B 88, 104103 (2013))



Some lithium thiophosphate crystal structures



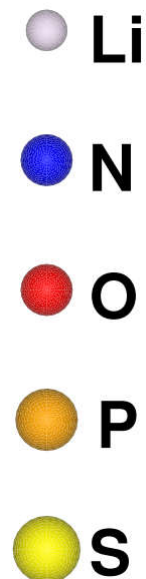
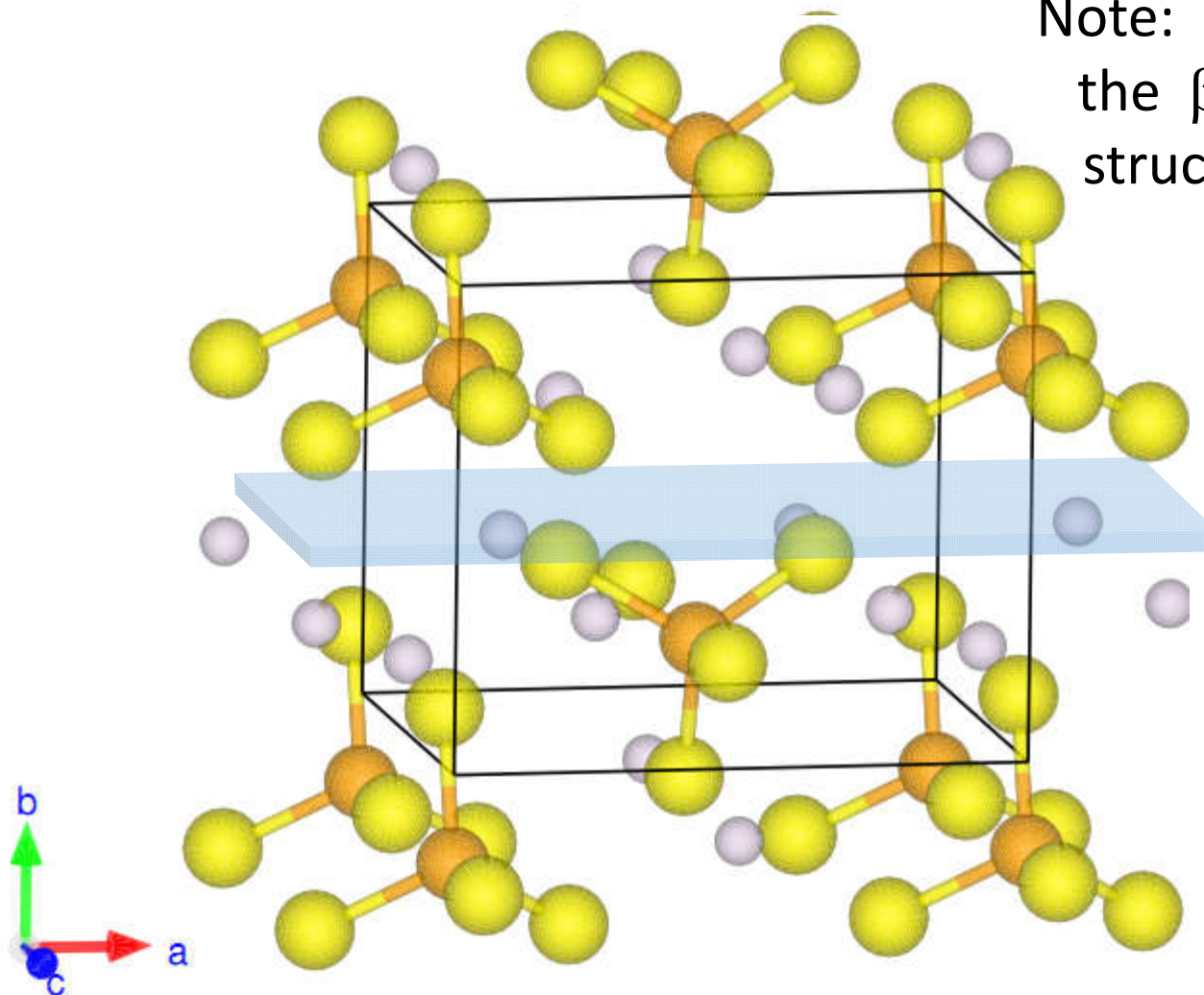
Experimentally amorphous;
computationally metastable
in $P\bar{1}$ structure



Experimentally and computationally
metastable in $P\bar{1}$ structure

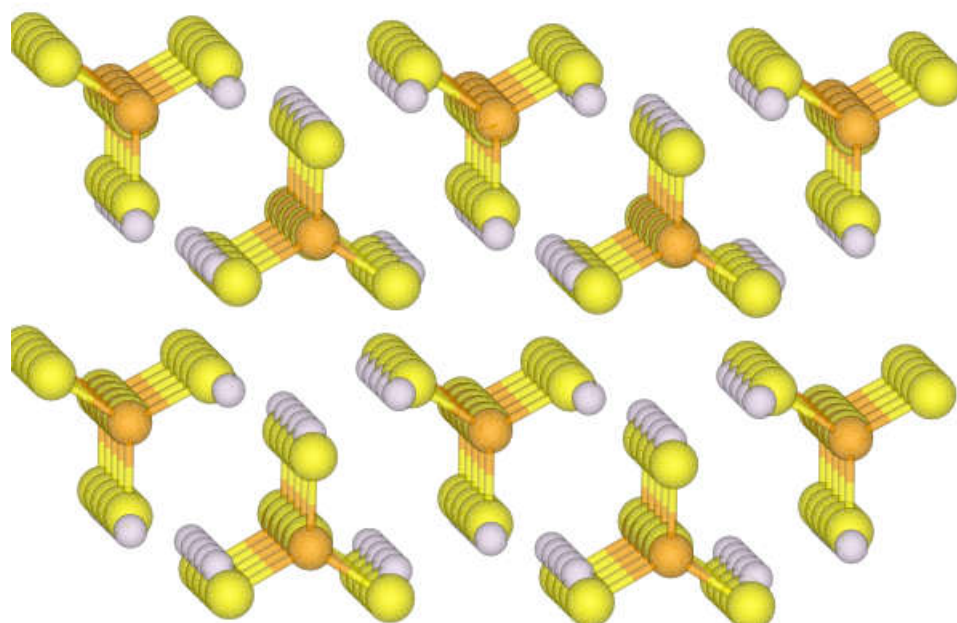
Crystal structure of bulk Li_3PS_4 – γ -form $\text{Pmn}2_1$ (#31)

Note: Li_3PS_4 is also found in the β -form with Pnma (#62) structure

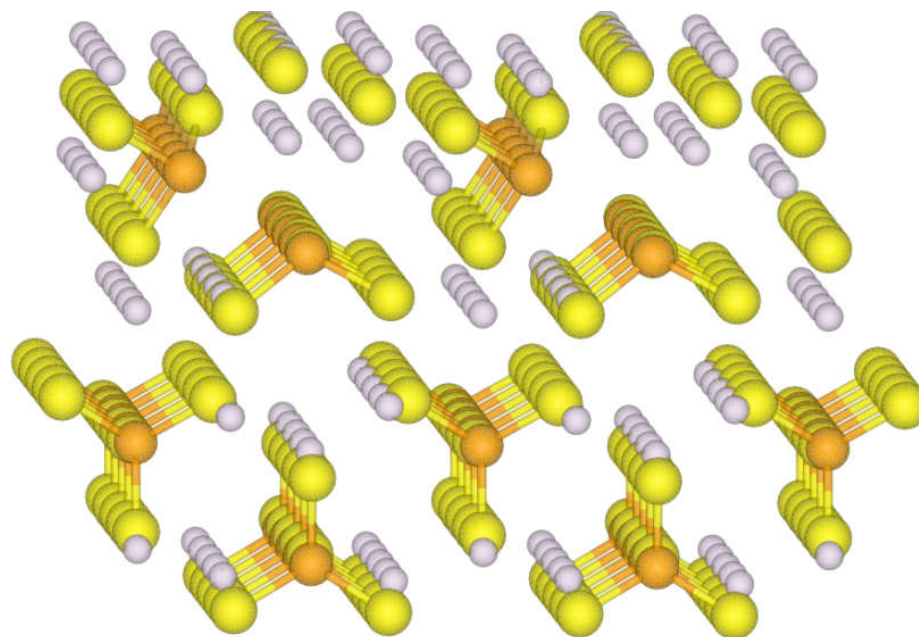


Simulations of ideal γ -Li₃PS₄ [0 1 0] surface in the presence of Li

Initial configuration:

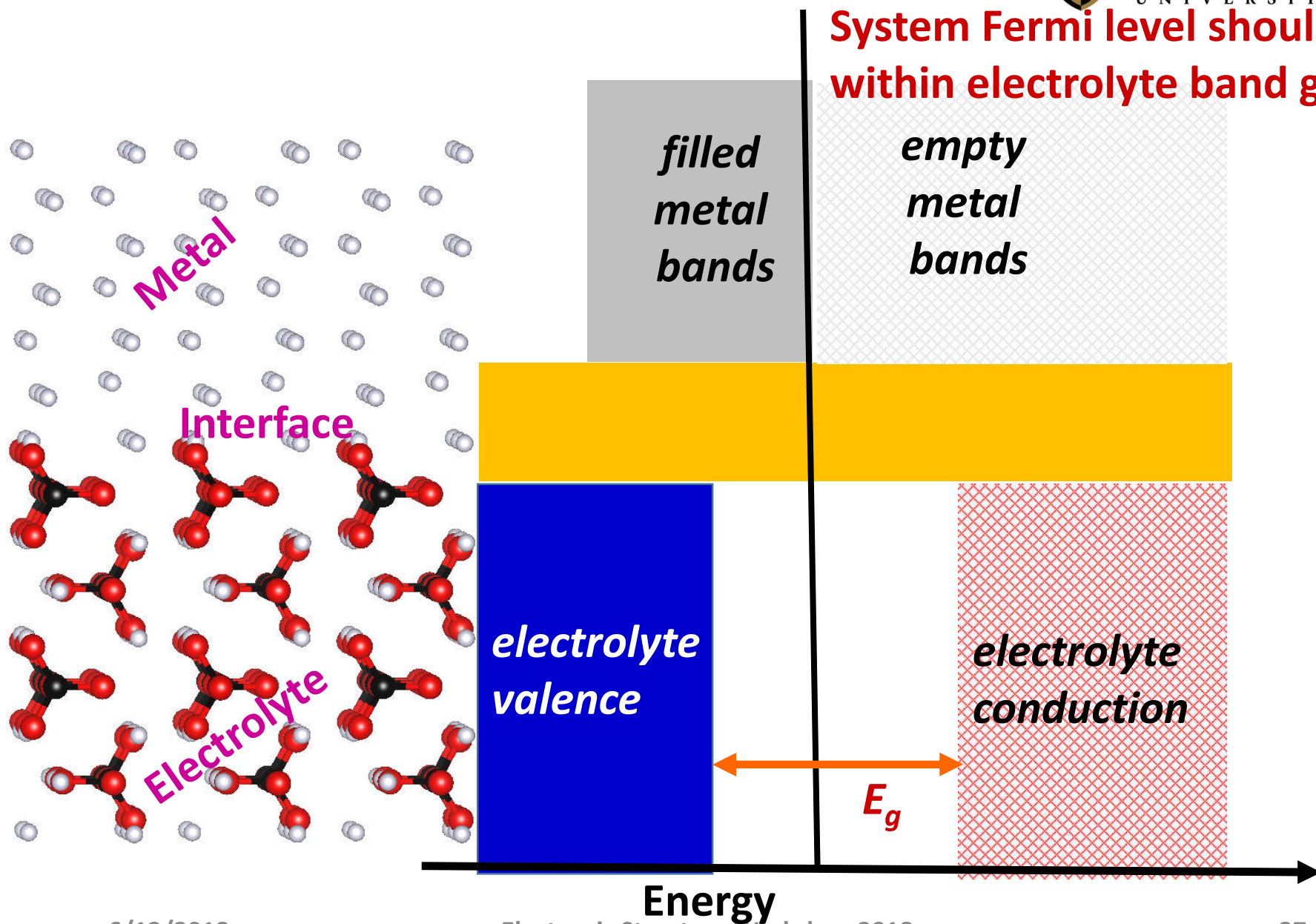


Computed optimized
structure:

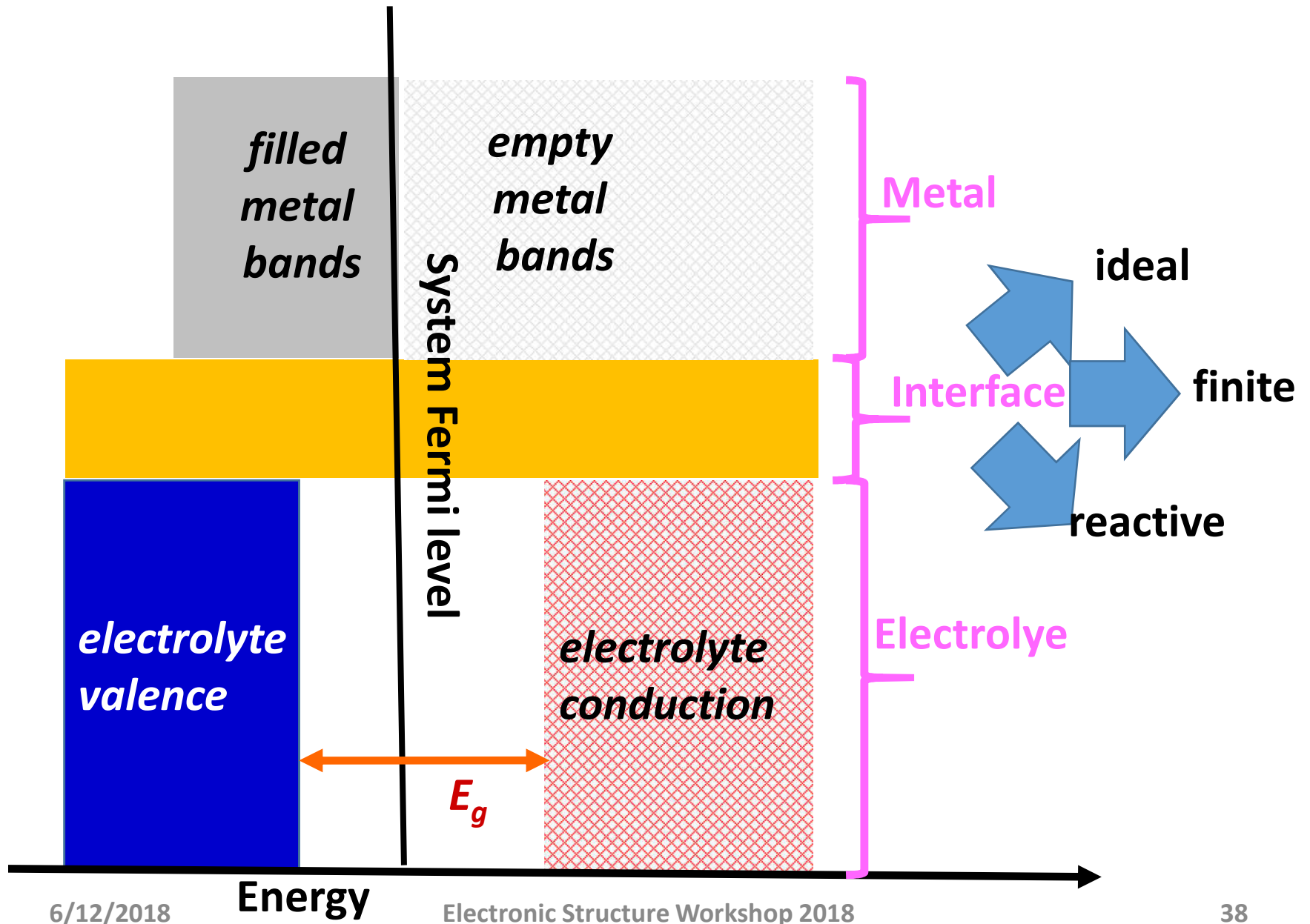


Energy diagram for ideal electrolyte/metal interface

System Fermi level should fall within electrolyte band gap.

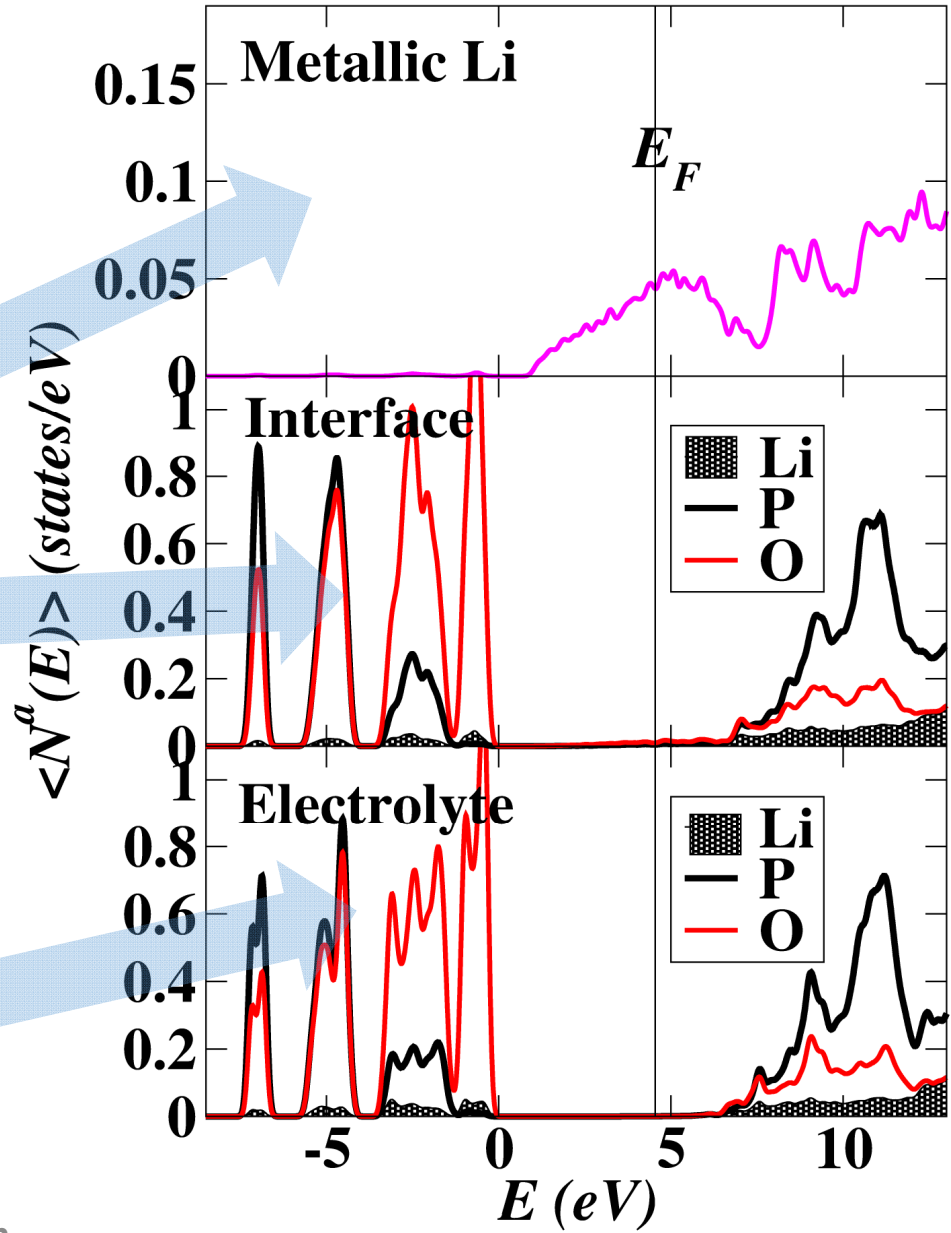
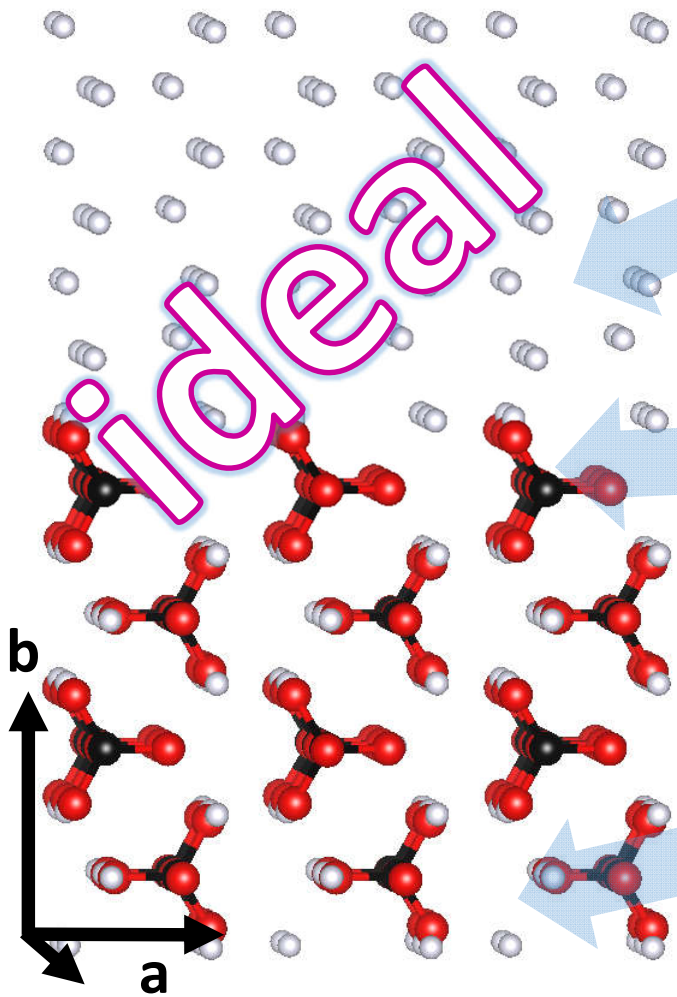


Possible interface configurations



γ -Li₃PO₄/Li system

Li P O
 ● ● ●

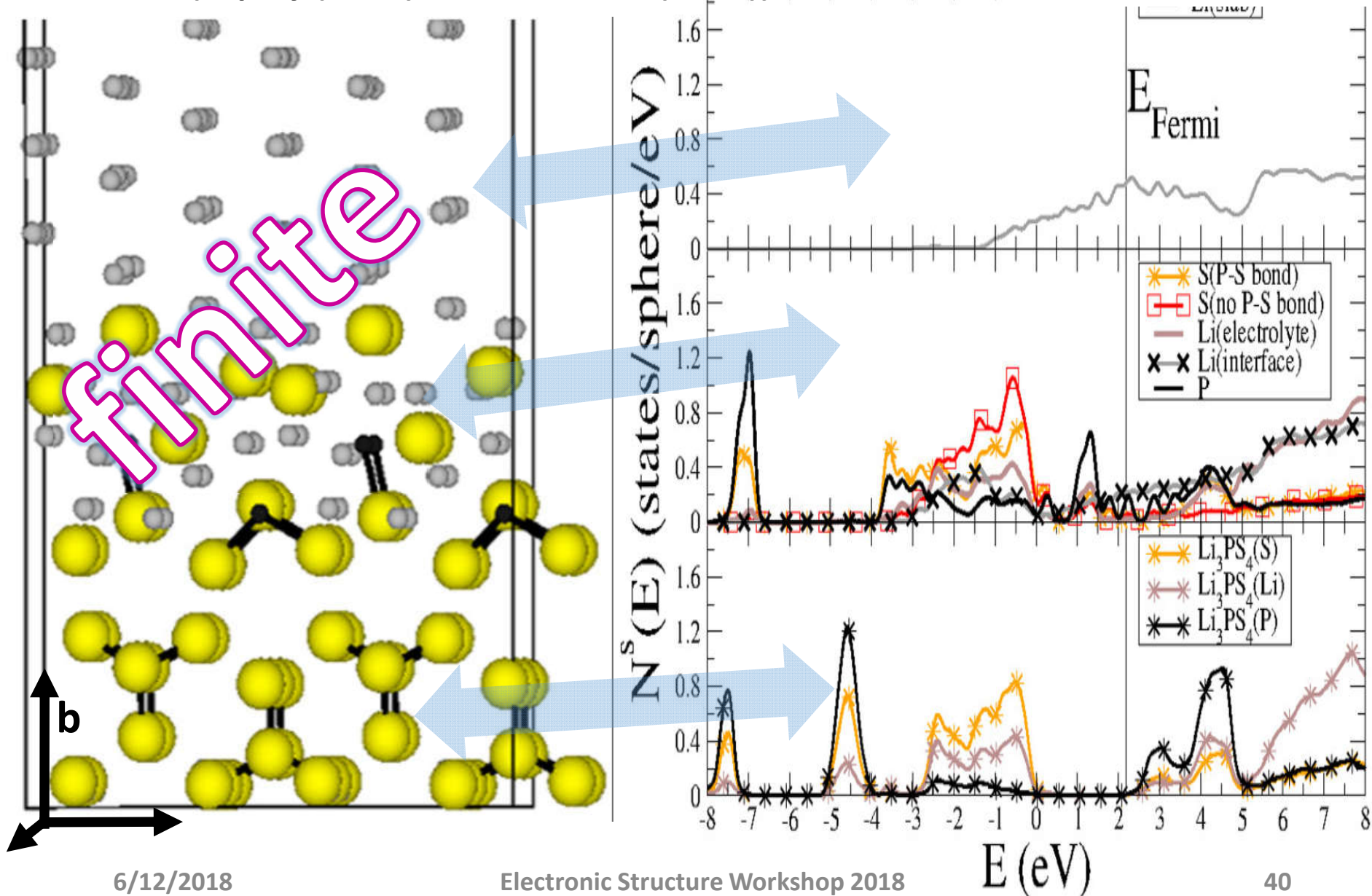


γ -Li₃PS₄/Li system

(Lepley *et al.*) PRB 92 21401 (2015)

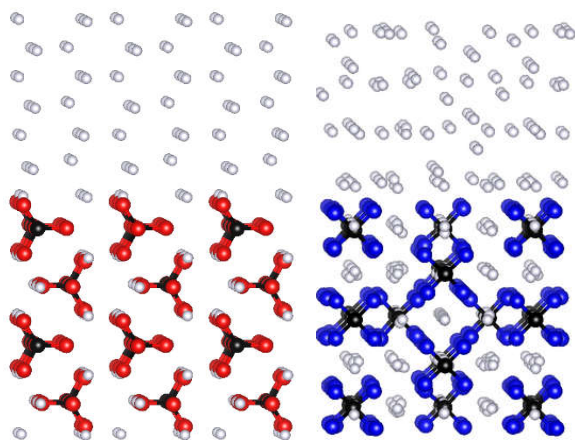


WAKE FOREST
UNIVERSITY



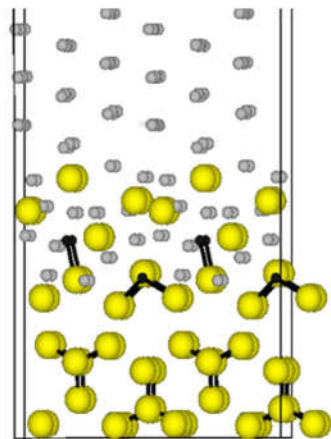
Summary of interface results

ideal

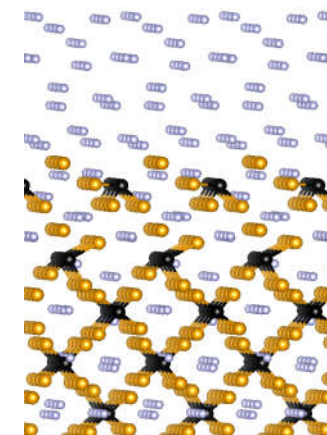


$\gamma\text{-Li}_3\text{PO}_4/\text{Li}$ $\text{Li}_7\text{PN}_4/\text{Li}$

finite



$\gamma\text{-Li}_3\text{PS}_4/\text{Li}$



$\text{Na}_3\text{SbS}_4/\text{Na}$

Thoughts on the role of simulations in developing battery technology

- Ideal research effort in materials includes close collaboration of both simulations and experimental measurements.
- For battery technology, there remain many opportunities for new materials development.